

**NASA TECHNICAL NOTE**



(NASA-TN-D-2051)

OTS: \$1.50

N64 11902\*

CODE-1

NASA TN D-2051

55 p.

<sup>T</sup>  
**COMPARATIVE EVALUATION OF  
METHODS FOR PREDICTING  
FLUTTER AND DIVERGENCE OF  
UNSWEPT WINGS OF FINITE SPAN**

by E. Carson Yates, Jr. and Samuel R. Bland

Auth: NASA  
Langley Research Center, 6021448

Langley Station, Hampton, Va.

Deposited: Washington, NASA, Dec. 1963 55 p refs

NATIONAL AERONAUTICS AND SPACE ADMINISTRATION • WASHINGTON, D. C. • DECEMBER 1963

**TECHNICAL NOTE D-2051**

**COMPARATIVE EVALUATION OF METHODS FOR PREDICTING FLUTTER  
AND DIVERGENCE OF UNSWEPT WINGS OF FINITE SPAN**

**By E. Carson Yates, Jr., and Samuel R. Bland**

**Langley Research Center  
Langley Station, Hampton, Va.**

**NATIONAL AERONAUTICS AND SPACE ADMINISTRATION**

# COMPARATIVE EVALUATION OF METHODS FOR PREDICTING FLUTTER

## AND DIVERGENCE OF UNSWEPT WINGS OF FINITE SPAN

By E. Carson Yates, Jr., and Samuel R. Bland

### SUMMARY

11902

Subsonic and supersonic flutter and divergence calculations have been made for five unswept wings by several analytical methods. The results have been compared with experimental flutter data in order to evaluate each method of predicting aeroelastic instabilities, particularly in the high subsonic and low supersonic to hypersonic ranges.

For the subsonic range, the methods examined included a modified strip analysis, two-dimensional loading modified to account for finite planform, and the subsonic kernel function. These methods all appeared to predict flutter speeds satisfactorily for Mach numbers below about 0.75 but, in the high subsonic range, the kernel-function method produced best agreement with experiment.

For the supersonic range, the methods examined included the modified strip analysis, modified two-dimensional loading, rectangular-wing theory, aerodynamic influence coefficients, and quasi-steady second-order theory. These calculations indicated that the use of linearized aerodynamic theory may lead to excessively unconservative estimates of flutter speeds even at relatively low supersonic Mach numbers. In contrast, aerodynamic theories which account for effects of finite wing thickness were indicated to be capable of predicting satisfactory flutter boundaries even into the hypersonic range. A simplified steady-state method, which represents the zero-frequency limiting case of the modified strip analysis, gave satisfactory flutter results in the subsonic and low supersonic to hypersonic ranges for a wing which fluttered at low reduced frequencies.

In the high subsonic range, divergence speeds calculated by modified strip analysis and by modified two-dimensional loading were indicated to be conservative.

Author

### INTRODUCTION

In the flutter analysis of unswept wings of moderate to high aspect ratios, a number of methods exist for evaluating the required distributions of subsonic and supersonic oscillatory aerodynamic loadings (refs. 1 to 31, for example). These methods involve varying degrees of approximation, and all are subject to theoretical preclusion at Mach numbers near 1.0. This limitation implies that

minimum flutter speeds, which generally occur in the transonic range, may not be adequately predicted by such methods. In contrast, for swept wings of moderate to high aspect ratio, flutter speeds can be predicted through the transonic range by approximate methods (ref. 4). Some applications of linearized potential-flow theory have been developed for Mach numbers near 1.0 (e.g., refs. 32 to 35), but because of approximations and complexity these procedures do not appear to be widely used in flutter analyses. The analysis of reference 32, for example, is restricted to low-aspect-ratio wings oscillating at low frequencies. Because of complications in the calculations, the method of reference 34, although pertinent to high-aspect-ratio wings, was applied only to rectangular wings oscillating without spanwise variation of motion or distortion.

The primary purpose of the present investigation is to examine, particularly in the high subsonic and low supersonic ranges, some results of modal-type flutter analyses employing various methods for evaluating the required oscillatory aerodynamic loading on unswept wings. The calculated flutter characteristics of five unswept wings are compared with existing experimental flutter data in order to evaluate each method of predicting flutter speeds in the vicinity of the transonic minimum values. In addition, for one of the wings, experimental data were available up to hypersonic Mach numbers. For that wing, the calculations are also extended into the hypersonic range in order to obtain comparisons over a wide range of Mach numbers between methods which include or exclude the effects of finite wing thickness. Since unswept wings may, in general, be subject to divergence as well as to flutter, divergence boundaries for the present wings were calculated by several of the methods employed in the flutter analyses.

In this investigation the methods employed for representing the oscillatory aerodynamic loading at Mach numbers less than 1.0 are a modified strip analysis, a simplified steady-state method, a modified two-dimensional loading (employing the loading parameters of refs. 9 and 10), and the kernel-function method. For Mach numbers greater than 1.0, the methods used are the modified strip analysis, the simplified steady-state method, the modified two-dimensional loading, a rectangular-wing theory, the finite-summation aerodynamic-influence-coefficient method, and the quasi-steady second-order theory. Piston theory is not included because reference 26 showed that at high Mach numbers piston theory and quasi-steady second-order theory give essentially the same results; whereas, at the lower supersonic Mach numbers, results of the quasi-steady second-order theory are the more conservative and are generally closer to experimental values. The transonic potential-flow methods are also excluded because of the limitations previously discussed.

## SYMBOLS

- A            aspect ratio of full wing including fuselage intercept
- $A_p$         aspect ratio of wing, considering side of fuselage as reflection plane  
            (twice panel aspect ratio)

$a_{c,n}$	nondimensional distance from midchord to local aerodynamic center (for steady flow) measured perpendicular to elastic axis, positive rearward, fraction of semichord perpendicular to elastic axis
$b$	wing semichord measured streamwise
$c_{l_{\alpha,n}}$	local lift-curve slope for section perpendicular to elastic axis in steady flow
$c_{m_{\alpha,n}}$	derivative with respect to angle of attack of local pitching-moment coefficient measured about leading edge of section perpendicular to elastic axis in steady flow
$e$	ratio of normal force coefficient measured in Freon-12 to normal force coefficient measured in air
$g$	structural damping coefficient
$M$	Mach number
$M_{\alpha,le}$	oscillatory section pitching moment measured about leading edge of wing section perpendicular to elastic axis
$\bar{m}$	total mass of wing panel
$P$	oscillatory section lift for wing section perpendicular to elastic axis
$t$	thickness of mounting shaft for wing 2001
$V$	flutter or divergence speed
$V_R$	reference flutter speed calculated from modified strip method by using aerodynamic parameters for two-dimensional incompressible flow
$v$	volume swept out by rotating rectangular wing about its midchord line
$\eta$	nondimensional coordinate measured from wing root along elastic axis, fraction of elastic axis length
$\lambda$	taper ratio of full wing including fuselage intercept
$\lambda_p$	taper ratio of exposed wing panel
$\mu$	mass ratio, $\bar{m}/\rho v$
$\rho$	free-stream fluid density
$\omega$	circular frequency of vibration at flutter
$\omega_i$	circular frequency of $i$ th natural (coupled) vibration mode

$\omega_{h,j}$       circular frequency of jth uncoupled bending vibration mode  
 $\omega_{\alpha}$       circular frequency of first uncoupled torsional vibration mode

Subscripts:

2D      two dimensional  
3D      three dimensional

## WINGS

### Wing Designation

For convenience the wing-designation system employed in references 1, 2, and 36 is retained in the present report. In the three-digit system used for the tapered wings, the first digit is the aspect ratio of the full wing to the nearest integer. The second and third digits give the quarter-chord sweep angle to the nearest degree. The letter R is appended to the planform designation in order to indicate a wing which has been ballasted to shift its local centers of gravity rearward. For the untapered wings the same designation system is used, except that a fourth digit 1 is appended to indicate the taper ratio.

### Wing Description

Some pertinent geometrical and structural parameters for the five wings are given in table I.

Wings 400 and 400R.- The two tapered wings treated in this report had aspect ratio 4.0, taper ratio 0.6, and NACA 65A004 airfoil sections. These wings, designated as wings 400 and 400R, were of essentially homogeneous construction and were ostensibly identical except where ballast weight was distributed along the trailing edge of wing 400R in order to alter the local center-of-gravity positions. (See fig. 1(a).) For flutter testing these wings were cantilever mounted in the midwing position on a cylindrical sting-fuselage with diameter equal to 21.9 percent of the span. The experimental flutter data and mass and stiffness properties for wing 400 are given in reference 36 and those for wing 400R are given in reference 1.

Wing 7001.- Wing 7001 is a homogeneous rectangular wing of aspect ratio 7.387. The airfoil of this wing varied linearly from an NACA 65A004 airfoil at the root to an NACA 65A002 airfoil at the tip. For flutter testing the wing was cantilever mounted in a midwing position on a fuselage of circular cross section. (See fig. 1(b).) Experimental flutter data and mass and stiffness properties for wing 7001 are given in reference 37. It should be noted that the experimental flutter data reproduced from reference 37 were obtained by several testing techniques with models of differing size. The present analyses, however, employed

only the physical properties of the wing models tested in the Langley transonic blowdown tunnel (data from ref. 37).

Wing 4001.- The rectangular wing panel with panel aspect ratio 1.73, called wing 4001, corresponds to a full wing of aspect ratio 4.00. This wing had 1.5-percent-thick symmetrical hexagonal airfoil section and was of solid steel construction. For flutter testing the wing was cantilever mounted from a half fuselage which was shimmed 0.25 inch from the tunnel floor in order to extend the model beyond the floor boundary layer. (See fig. 1(c).) Experimental flutter data and mass and stiffness properties for wing 4001 are given in reference 38.

Wing 2001.- The square wing panel (wing 2001) corresponds to a full rectangular wing with aspect ratio 2.00 and with 9-percent-thick symmetrical diamond airfoil section. The wings which were flutter tested were built on a core of stainless-steel sheet with an integral rectangular shaft for mounting. (See fig. 1(d).) The airfoil contour was formed by balsa wood cemented to the metal core. The cores were perforated and ballasted in order to maintain essentially constant inertia properties and frequency ratios for three different levels of mounting-shaft stiffness. For flutter testing these wings were mounted by clamping the end of the shaft at the tunnel wall as shown in figure 1(d). The semicylindrical fairing shown was used for transonic testing but was replaced by a reflection plane for supersonic testing. The experimental flutter data and mass and stiffness properties for wing 2001 are given in reference 39.

### Vibration Mode Shapes and Frequencies

Mode shapes.- Uncoupled vibration modes were employed in flutter calculations for all five wings. For wings 400, 400R, 7001, and 4001, calculated cantilever-beam modes for the first torsion and first and second bending modes were used. Unlike the other four wings, wing 2001 was not cantilevered at the root; hence, the term "uncoupled modes" has a somewhat different connotation for this wing. For wing 2001, the "uncoupled modes" are taken to be rigid-body modes for the wing panel in pitch and in flapping; these modes were calculated and given in reference 39. In addition to these modes, the first two measured natural (coupled) modes for wing 2001 were also available from reference 39, and they were used in some flutter calculations.<sup>1</sup> These coupled modes contain some torsional deformation of the wing panel which, of course, is not included in the rigid-body uncoupled modes.

Modal frequencies.- With the exception of the rigid-body frequencies which were calculated for wing 2001, all modal frequencies used herein were obtained from measured values. Since wings 400, 400R, 7001, and 4001 are cantilevered, unswept, and of moderate to high aspect ratio, their natural-mode frequencies would be expected to differ little from their uncoupled-mode frequencies, at least in the lower modes. Accordingly, following the procedure used in reference 40, the measured natural-mode frequencies for these four wings are used

---

<sup>1</sup>The mode shape for the third natural mode is not given in reference 39. However, its omission from the flutter calculations should have an insignificant effect on the resulting flutter speeds because the third-mode frequencies were shown to be at least 2.5 times the second-mode frequencies.

directly as uncoupled-mode frequencies. The corresponding measured torsion-mode frequencies were "uncoupled" by means of the relation used in reference 40. The resulting uncoupled torsion-mode frequencies differ from the measured values by an insignificant amount.

All the modal frequencies used in the flutter calculations are summarized in table I.

## FLUTTER AND DIVERGENCE CALCULATIONS

### General Considerations

The types of flutter and divergence calculations performed in this investigation are summarized in table II. In all calculations for wings 400, 400R, 7001, and 4001, a single representative value of flow density was used for each wing as in references 1 and 2 (see table I herein), because the large number of experimental flutter points for each of these wings were obtained at different densities. The flutter points measured for wing 2001, however, were relatively few, and they covered a considerably greater range of Mach number. Therefore, each calculation for wing 2001 employed the value of flow density associated with the nearest experimental flutter point. In particular, all subsonic calculations for wing 2001 included the flow density for the flutter point measured at the lowest Mach number ( $M = 0.97$ ). Some effects of varying flow density are discussed in references 2, 41, and 42.

The transonic flutter data for wing 2001 were measured in Freon-12 rather than in air (ref. 39). Reference 41 pointed out that flutter-speed boundaries for Freon-12 are slightly lower than corresponding boundaries for air at the same density and Mach number because aerodynamic load intensities (e.g., section lift-curve slopes) are greater in Freon-12 than in air. This difference in loading has been accounted for in order to make the calculated flutter characteristics more directly comparable to the experimental data. For all calculations corresponding to flutter data measured in Freon-12, the load intensities have been obtained by effectively increasing corresponding loads for air by a Mach number dependent factor which ranged from 1.0 at  $M = 0$  to about 1.1 in the transonic range. The magnitude of this factor was based on the extensive comparisons of load-distribution measurements in air and in Freon-12 shown in figure 16 of reference 43. This type of load modification is discussed in more detail in reference 41.

Finally, very little information was available with regard to values of the modal structural damping coefficients for the five wings investigated. However, damping-coefficient values for the lower modes of homogeneous wings such as wings 400, 400R, 7001, and 4001 are generally very low. Also, damping for wing 2001 should be very small because the predominant portion of the vibrational deformation occurred in the solid metal mounting shaft. Consequently, in most of the present flutter calculations the flutter points were considered to be defined by conditions requiring zero structural damping to sustain constant-amplitude oscillations. A few calculations, however, included arbitrary but small nonzero values



of structural damping. In all cases the damping values were taken to be the same for all modes.

### Methods of Analysis

As indicated previously, a number of methods exist for evaluating the oscillatory aerodynamic loads required in the flutter analysis of unswept wings in compressible flow. (See refs. 1 to 31, for example.) Several of these methods which are employed in the present investigation are described briefly in the following section. Some variations applied herein to two of the methods, namely the simplified steady-state method and the modified two-dimensional loading, are discussed in somewhat more detail.

Modified strip analysis.- The modified-strip-analysis method of flutter prediction was presented in reference 1, extended in references 3 and 4, and further applied in references 2, 41, and 42. In this method, spanwise distributions of steady-flow section lift-curve slope and local aerodynamic center for the undeformed wing are used in conjunction with the "effective" angle-of-attack distribution resulting from the assumed vibration modes in order to obtain values of section lift and pitching moment. The steady-state aerodynamic parameters may be obtained from any suitable theory or experiment, the criterion being that the best method to use is the one that yields the most accurate steady-state load distributions. Circulation functions modified on the basis of loadings for two-dimensional airfoils oscillating in compressible flow are employed to account for the effects of oscillatory motion on the magnitudes and phase angles of the lift and moment vectors.

Since the required distributions of section lift-curve slope and local aerodynamic center may be obtained in any desired manner, for the present calculations they were obtained from subsonic and supersonic linearized three-dimensional potential-flow theory (lifting-surface theory) as in references 1 and 2, from modification of the supersonic linear-theory values based on two-dimensional shock-expansion theory as in reference 3, and from transonic wind-tunnel and supersonic flight tests as in reference 4. (See table II.) Some of the particular values used herein for wings 400, 400R, 7001, and 4001 are given in references 1 and 4, and in figures 2 and 3 of the present report. Figures 2 and 3 also include for comparison the corresponding values from subsonic lifting-line theory which were used in the flutter calculations of references 1 and 2. For wing 4001, use of shock-expansion theory at  $M = 1.3$  and  $M = \sqrt{2}$  yielded values of section lift-curve slope which were less than 2 percent greater than corresponding linear-theory values; the local aerodynamic centers obtained from shock-expansion theory were less than 2-percent chord forward of the corresponding positions indicated by linear theory. The steady-flow aerodynamic parameters required for wing 2001 (fig. 4) were calculated from subsonic and supersonic linearized lifting-surface theory and for the higher supersonic Mach numbers from linearized theory with a modification based on shock-expansion theory as in reference 3. The resulting modified distributions of local aerodynamic center are included in figure 4, but the altered section lift-curve slopes are very close to the corresponding linear-theory values and hence are not shown.

Although the modified strip analysis is applicable to swept wings at transonic speeds (ref. 4), it was indicated in reference 1 to be unsuitable when the component of Mach number normal to the leading edge is near 1.0 because of the nature of the circulation functions employed. Thus the method is not usable for unswept wings in the transonic range. The present calculations, in addition to those of reference 4, supply some quantitative information on the extent of this inaccessible range. Applications extending into the hypersonic range are also shown for wing 2001. It is believed, however, that the aspect ratio of wing 2001 is probably fairly close to the minimum for which any strip method may reasonably be used at subsonic and low supersonic Mach numbers.

Simplified steady-state method.- The simplified steady-state method was presented in reference 5 and applied with some variations in references 6 and 7. This method may be derived from the modified strip analysis by ignoring all unsteady aspects of the aerodynamic loading and by neglecting all aerodynamic terms which result from bending motions. The only remaining aerodynamic input to the wing is a steady-state (pure real) loading which is associated with the instantaneous pitch angle (or angle of attack) of each wing section. Hence, this method coincides with the zero-frequency limiting case of the modified strip analysis and may be employed for any Mach number for which accurate steady-state load distributions are available.

Such a method would, of course, be expected to yield reasonable flutter results only when flutter occurs at very low reduced frequencies. This condition frequently exists in the supersonic to hypersonic range, but reduced frequencies often reached maximum values in the transonic range. On the other hand, the transonic limitation for unswept wings, mentioned previously in connection with the modified strip analysis, does not apply to the simplified steady-state method because circulation functions are neglected. In the present application to wing 2001, however, Mach numbers very near 1.0 are not included because measured values of section lift-curve slope and local aerodynamic center were not available, and because the accuracy of steady-state potential theory is questionable near sonic speeds.

Modified two-dimensional loading.- Another strip type of approach is to use aerodynamic coefficients for two-dimensional oscillating wings in a section-by-section application across the span of a finite wing. In a procedure of this sort, finite-span effects may be accounted for approximately by weighting the two-dimensional oscillatory coefficients on the basis of three-dimensional steady-state loading. References 9 and 10 give tabulated values of loading coefficients for two-dimensional thin wing sections oscillating without deformation in compressible flow. These coefficients, derived from subsonic, transonic, and supersonic linearized unsteady potential-flow theory, are applied herein to wings of finite span by weighting the oscillatory two-dimensional section lift and pitching moment on the basis of section lift and pitching-moment coefficients calculated from linearized three-dimensional steady-flow theory. Thus, for each wing section

$$P_{3D,unsteady} = P_{2D,unsteady} \frac{(c_{l\alpha,n})_{3D,steady}}{(c_{l\alpha,n})_{2D,steady}}$$

and

$$(M_{\alpha,le})_{3D,unsteady} = (M_{\alpha,le})_{2D,unsteady} \frac{(c_{m\alpha,n})_{3D,steady}}{(c_{m\alpha,n})_{2D,steady}}$$

where  $P_{2D,unsteady}$  and  $(M_{\alpha,le})_{2D,unsteady}$  are, respectively, the section lift and pitching moment given by the two-dimensional linearized potential-flow theories of references 9 and 10; in all cases  $(c_{l\alpha,n})_{2D,steady}$  and  $(c_{m\alpha,n})_{2D,steady}$  are, respectively, the well-known section lift-curve slope and section pitching-moment-curve slope given by two-dimensional steady-flow theory which corresponds to the zero-frequency limit for the theories of references 9 and 10, that is,

$$(c_{l\alpha,n})_{2D,steady} = \frac{2\pi}{\sqrt{1 - M^2}} \quad (M < 1)$$

$$= \frac{4}{\sqrt{M^2 - 1}} \quad (M > 1)$$

and

$$(c_{m\alpha,n})_{2D,steady} = \frac{\pi}{2\sqrt{1 - M^2}} \quad (M < 1)$$

$$= \frac{2}{\sqrt{M^2 - 1}} \quad (M > 1)$$

Flutter calculations for all five wings were made with spanwise distributions of  $(c_{l\alpha,n})_{3D,steady}$  and  $(c_{m\alpha,n})_{3D,steady}$  obtained from subsonic (ref. 44) and supersonic (ref. 45) linearized potential-flow theory. (See table II.) In addition, some supersonic flutter calculations for wing 2001 employed values of  $(c_{l\alpha,n})_{3D,steady}$  and  $(c_{m\alpha,n})_{3D,steady}$  which were modified by shock-expansion theory as in reference 3 in order to take approximately into account the effect of finite wing thickness. Finally, for comparison, the two-dimensional linear-theory loadings of references 9 and 10 were employed without alteration in some calculations for wings 400 and 7001. (See table II.)

These procedures are, of course, strip methods and hence are subject to the usual planform limitations that apply to such methods, as discussed in

reference 1, for example. The present methods, however, are not restricted to unswept wings but could be extended to swept wings by applying the previously described expressions to wing sections normal to the elastic axis as in the modified strip analysis (ref. 1). Use of a steady-state type of modification such as the one employed here is questionable if the flutter reduced frequency  $b\omega/V$  is high. On the other hand, at Mach numbers near 1.0 the aerodynamic coefficients obtained from two-dimensional linearized potential-flow theory are of questionable validity for low reduced frequencies. The present procedure may therefore prove to be of limited value in the transonic range, even if measured steady-flow parameters were used in the modification.

Subsonic kernel function.- The subsonic kernel-function flutter calculations were based on the method described in reference 12 (see also ref. 11) which was derived from three-dimensional linearized unsteady potential-flow theory. In order to calculate the pressure distribution on an oscillating wing from the integral equation which relates pressure and downwash, the method of reference 12 employs a collocation procedure. In this procedure the lifting pressure is considered to be composed of a linear combination of a number  $n$  of assumed pressure modes. The forms of the pressure modes are chosen so that the boundary conditions at the leading edge, trailing edge, and tip are satisfied. The  $n$  arbitrary coefficients in the linear combination of pressure modes are evaluated by requiring the pressure-induced downwash to equal that resulting from the wing deflection at  $n$  discrete collocation points on the wing surface.

In all calculations the wing root was considered to be a reflection plane, and the nine downwash collocation points used were located chordwise at 25, 50, and 75 percent of the local chord. Wings 400 and 400R were cantilevered at the root, so the collocation points were taken at 30, 60, and 90 percent of the panel span in order to evaluate the aerodynamic loading most accurately over the outboard portions of these wings where the greatest deflections occurred. However, some unpublished calculations for wing 400 have indicated that the calculated flutter characteristics are not very sensitive to small changes in the spanwise positions of the collocation points. Wing 2001 was not cantilevered at the root, and significant deflection of the root occurred in both of its measured natural vibration modes as well as in its rigid-body pitching and flapping modes. Hence, in order to obtain a reasonably accurate evaluation of the aerodynamic loading over the entire wing panel, the collocation points for wing 2001 were taken at 20, 50, and 80 percent of the panel span.

Rectangular-wing theory.- The rectangular-wing theory of reference 13 (see also refs. 14 to 18) is based on a development of the velocity potential for supersonic flow near the corner of a quarter-infinite thin wing undergoing harmonic motion of small amplitude with arbitrary deflection shape. The solution to this linearized boundary-value problem is obtained by means of integral transform techniques and is expressed in terms of integrals over a portion of the wing area. This method has been applied (ref. 17) to the calculation of oscillatory section lift and pitching-moment coefficients for wings with deflection shapes that are linear in the chordwise coordinate and monomial (single-power term) in the spanwise coordinate. The equations of reference 17 have been employed herein in flutter calculations for wings 7001, 4001, and 2001. The cantilever-beam (uncoupled) modes for wings 7001 and 4001 as well as the rigid-body modes and natural modes

for wing 2001 are linear in the chordwise variable so that the chordwise-deflection-shape restriction of reference 17 imposes no additional approximation. However, spanwise variations of the mode shapes for these wings were approximated by polynomials, and the expressions of reference 17 were applied for each monomial term. For wings 7001 and 4001, the first torsion mode and the first and second bending modes were approximated, in the least-squares sense, by polynomials of third, fourth, and fifth degrees, respectively. For wing 2001 both the rigid-body modes and the natural modes, given in reference 39, are linear in the spanwise variable.

In addition to the usual limitations of linearized aerodynamic theory, the rectangular-wing theory is also limited to Mach numbers for which no Mach line from the wing tip intersects the root chord. Hence, it is not generally applicable for Mach numbers near 1.0.

Aerodynamic influence coefficients.- The aerodynamic-influence-coefficient method of references 19 to 21 is based on the linearized velocity potential for an oscillating wing in supersonic flow. The oscillatory lifting pressure on the wing is expressed as a surface integral of the product of the oscillatory downwash and the influence function. The downwash, in turn, is evaluated from the frequency and the vibration mode shape, and the influence function is derived from the properties of simple flow singularities. In general, the lifting-pressure integral cannot be evaluated in closed form, so that a finite-summation approximation is employed for its computation. For this purpose the wing surface is divided into small but finite areas or "boxes," and the influence function is approximated in each box by its value at the box center. For the present calculations the boxes were taken to be rectangles with diagonals parallel to the Mach lines. The advantages and disadvantages of several different shapes of boxes are discussed in references 19 to 23. Regardless of the shape of the boxes, however, their size must be decreased and their number increased until convergence of the flutter solution is indicated. If convergence is achieved and if the reduced frequency is small, the influence-coefficient method should yield essentially the same flutter results for rectangular wings as the previously mentioned rectangular-wing theory. The aerodynamic-influence-coefficient method was therefore used in flutter calculations for only one wing (wing 4001). (See table II.)

Quasi-steady second-order theory.- The quasi-steady second-order theory employed herein and in references 25, 26, and 42 is based on the supersonic steady-flow second-order theory of reference 24. The lifting-pressure expression of reference 24 (see also ref. 25) is used to represent the pressure distribution on an oscillating wing as if it were composed of a succession of steady-state distributions each associated with an instantaneous angle of attack. This procedure is reasonable for high Mach numbers because the flutter reduced frequency generally decreases as Mach number increases. Thus, at high Mach numbers the unsteady aspects of the flow have reduced significance.

The lifting-pressure expression for quasi-steady second-order theory (ref. 25) differs from that for second-order piston theory only with regard to two coefficients that are functions of Mach number and the ratio of specific heats. Furthermore, as Mach number approaches infinity, the lifting-pressure

expressions for the two theories approach each other. Both theories permit the inclusion of airfoil shape, and this was accounted for in the present calculations. As indicated in references 25 and 26, the flutter results of these two theories are generally similar, with the quasi-steady second-order theory usually yielding the better agreement with experiment at the lower supersonic Mach numbers. Therefore, piston theory has not been included in the flutter comparisons of the present report.

Neither quasi-steady second-order theory nor piston theory take formally into account the aerodynamic effects of streamwise wing tips. However, in all of the flutter calculations for wing 2001 an approximate tip correction was made (as in refs. 26 and 42) on the basis of steady-flow linear theory. This tip correction consists of multiplying the second-order-theory loading at each point on the wing by the ratio of steady-state load (ref. 45) for the wing with streamwise tip to steady-state load for the wing without streamwise tip. The correction alters the aerodynamic loading only within the triangular region influenced by the tip, and it is, of course, a reasonable approximation only for low reduced frequencies.

## PRESENTATION OF RESULTS

Results of the flutter and divergence calculations for the five unswept wings (table II) are compared with experimental flutter data in figures 5 to 10. To facilitate comparisons with previously published results, flutter and divergence speeds for all the wings are presented in the form of a speed ratio  $V/V_R$ .

In this ratio the normalizing reference speed  $V_R$  for each theoretical or experimental point is the flutter speed calculated by the modified-strip method, with the density associated with the numerator  $V$  and with aerodynamic parameters for two-dimensional incompressible flow ( $c_{l\alpha,n} = 2\pi$  and  $a_{c,n} = -\frac{1}{2}$ ). For wing 2001, all values of  $V_R$  were calculated with rigid-body vibration modes. In addition to the flutter-speed and divergence-speed ratios, the results for wing 2001 are also presented in the form of a flutter-speed and divergence-speed index  $\frac{V}{b\omega_\alpha\sqrt{\mu}}$

(figs. 9(b) and 10(b)) in order to show that the two types of graph differ only slightly for an unswept wing which flutters at low reduced frequencies. In contrast, reference 42 showed that these types of graph may differ noticeably for a swept wing which flutters at relatively higher reduced frequencies.

All flutter frequencies are normalized with respect to the uncoupled-torsion-mode frequency  $\omega_\alpha$ . The calculated flutter frequencies given in figures 5 to 8 do not show the transonic discontinuities usually exhibited by the calculated flutter speeds. Therefore, where both subsonic and supersonic flutter frequencies have been calculated by the same method, the resulting frequency curves have been faired through the transonic range.

Unless otherwise indicated, all calculated flutter points are defined by conditions for zero structural damping ( $g = 0$ ).

## DISCUSSION OF FLUTTER RESULTS

### Subsonic Speed Range

Modified strip analysis.- For wings 400, 400R, 7001, and 4001 (figs. 5 to 8), subsonic flutter speeds calculated by the modified strip analysis are in good agreement with the few available experimental data points for Mach numbers up to 0.85. For wings 7001 and 4001, however, the calculated flutter-speed curves turn upward at Mach numbers around 0.80 and thus begin to deviate from the experimental trend. Reference 4 indicated that because of the behavior of the circulation functions employed, flutter speeds calculated for unswept wings increase without limit as  $M$  approaches 1.0. Although reference 4 showed that this asymptotic increase of calculated flutter speed was eliminated by use of measured steady-flow aerodynamic parameters, the resulting flutter speeds were still not in satisfactory agreement with experimental values. It is therefore unlikely that use of measured aerodynamic parameters as in reference 4 would result in any significant or consistent extension of the  $0 \leq M \leq 0.85$  range of usefulness for applying the modified strip analysis to unswept wings. In contrast, reference 4 illustrated satisfactory application of the method to swept wings through the transonic range.

For wing 2001, subsonic experimental data are not available for comparison with results of the modified strip analysis, but the calculated subsonic flutter speeds are somewhat higher than the measured values at Mach numbers near 1.0 (fig. 9(a)). However, these calculations employed rigid-body vibration modes. Use of the natural vibration modes, which contain some torsional deformations not represented by the rigid-body modes, would be expected to yield some reduction of calculated flutter speed as it did in the case of calculations by the simplified steady-state method and by the kernel-function method (fig. 10(a)).

The subsonic flutter frequencies obtained from the modified strip analysis (figs. 5 to 9) show little variation with Mach number and compare satisfactorily with experimental values.

Simplified steady-state method.- The simplified steady-state method was employed only for wing 2001 (figs. 9 and 10). Subsonic flutter speeds calculated by this method with rigid-body modes and with aerodynamic parameters obtained from linearized theory decrease monotonically with increasing Mach number and are in good agreement with transonic experimental values (fig. 9). At  $M = 0$ , the simplified steady-state method and the modified-strip-analysis method yield essentially coincident flutter speeds. At higher Mach numbers the simplified steady-state method predicts the lower flutter speeds primarily because the "circulation function" associated with that method is  $1 + i0$  for all reduced frequencies and Mach numbers. Therefore, as  $M$  approaches 1.0, flutter speeds calculated by the simplified steady-state method do not rise asymptotically as do those given by the modified strip analysis.

Subsonic flutter speeds calculated by the simplified steady-state method with natural vibration modes are about 18 percent lower than those obtained with rigid-body modes and, in comparison with experiment at Mach numbers near 1.0, appear to be about 10 to 15 percent conservative (fig. 10). It should be remembered, however, that accuracy of flutter prediction with this method requires the flutter reduced frequency to be low. This condition is satisfied for wing 2001 which is an all-moving surface, but, for cantilevered surfaces, reduced-frequency values might not, in general, be small enough to yield acceptably accurate flutter speeds, particularly in the subsonic and low supersonic ranges.

Modified two-dimensional loading.- For all five wings flutter speeds calculated by use of modified two-dimensional loading are close to values given by the modified strip analysis at the lower subsonic Mach numbers ( $M < 0.75$ ). For wing 400, however, the flutter speeds obtained with modified two-dimensional loading increase monotonically with increasing Mach number, contrary to the usual experimental trend and contrary to the trend indicated by the modified strip analysis and by the subsonic kernel-function method (fig. 5). Moreover, strip-theory-type flutter calculations employing two-dimensional loading coefficients without modification for finite span (fig. 5) indicated that the extensive upturn of the flutter-speed curve at the higher subsonic Mach numbers is not caused by the finite-span modification. At the higher subsonic Mach numbers, flutter speeds obtained by use of modified two-dimensional loading become appreciably higher than experimental values. The calculations of reference 46, which employed unmodified two-dimensional loading, showed a similar upturn of calculated flutter speed as Mach number approached 1.0. In contrast, corresponding flutter speeds calculated for wing 400R (fig. 6) decreased as Mach number increased to 0.95 and were in good agreement with experimental flutter-speed levels up to  $M = 0.99$ . Subsequent calculations showed that this difference in calculated flutter speed between wings 400 and 400R was caused primarily by their different section center-of-gravity locations. Differences in section mass and moment of inertia in pitch had little effect, and the differences in modal frequency ratios and flow density for these two wings had negligible effect on the shape of the calculated flutter-speed curves.

For wings 7001 and 4001, flutter speeds calculated by use of modified two-dimensional loading are in good agreement with experimental values up to Mach numbers above 0.90 (figs. 7 and 8). For wing 2001, however, the calculated values become excessively conservative at the higher subsonic Mach numbers (fig. 9).

Flutter frequencies calculated with modified two-dimensional loading compare satisfactorily with the available measured values for all five wings.

Subsonic kernel function.- Both flutter speeds and frequencies calculated by the subsonic kernel-function method for wings 400 and 400R (figs. 5 and 6) are in good agreement with experimental values for Mach numbers up to at least 0.95. However, some similar calculations (unpublished) for swept wings have indicated that under some conditions the agreement may be less satisfactory, particularly at Mach numbers near 1.0. In fact, for Mach numbers approaching 1.0, especially when reduced frequencies are small, any linearized aerodynamic theory should probably be used with caution because the nonlinear effects of viscosity, mixed flow regions, and shock waves may significantly influence aerodynamic loadings.



For wing 2001, flutter speeds obtained from the kernel-function method at the higher subsonic Mach numbers essentially coincide with values given by the simplified steady-state method (figs. 9 and 10). When rigid-body vibration modes are used in the calculations, the results of both methods are in very good agreement with measured flutter speeds at Mach numbers up to 0.99. However, when measured natural modes are used, the calculated flutter speeds are slightly conservative.

### Supersonic Speed Range

Modified strip analysis.- Supersonic flutter speeds calculated for all five wings by the modified strip analysis with aerodynamic parameters obtained from linearized theory are unconservative by amounts varying from a few percent for wing 400R (fig. 6) to about 140 percent for wing 400 (fig. 5). Reference 2 showed that, for wings 400, 400R, 7001, and 4001, these unconservative results were associated with two conditions: (1) Flutter speeds given by the modified strip analysis become very sensitive to small changes in local aerodynamic center, which appears explicitly in the flutter equations, when the local aerodynamic centers lie close to the local centers of gravity and (2) Linearized aerodynamic theory characteristically predicts aerodynamic centers that are too far aft. For example, reference 2 showed that a forward shift of only 1-percent chord in the local aerodynamic-center locations for wing 7001 reduced the calculated supersonic flutter speeds to levels that agreed well with the experimental data. Furthermore, reference 4 and figures 5 and 6 show that the use of measured aerodynamic parameters greatly improved calculated results for wing 400 and produced excellent agreement with experimental flutter speeds and frequencies for wing 400R.

For wing 4001, use of aerodynamic parameters given by shock-expansion theory reduced calculated flutter speeds considerably below values obtained with linearized aerodynamic theory (fig. 8), but the reduction does not appear to be sufficient to yield close agreement with experiment. Use of shock-expansion theory for wing 2001 (fig. 9) reduces flutter speeds calculated with rigid-body modes to about two-thirds of the values obtained with linear-theory aerodynamic parameters and results in accurate representation of experimental trends, although calculated flutter-speed levels remain somewhat high. Although measured structural-damping values were not available for wing 2001, the modified-strip-analysis calculations which included finite wing thickness (aerodynamic parameters obtained from shock-expansion theory) for this wing indicated that inclusion of a small amount of structural damping would decrease slightly the calculated supersonic flutter speeds shown in figure 9. For example, at  $M = 6.86$ , an increase in  $g$  from 0 to 0.01 would decrease the calculated flutter speed by about 4.5 percent. Reference 47 has shown that under some conditions structural damping may have an adverse effect on flutter speeds calculated by piston theory for hypersonic Mach numbers. Shock-expansion theory, however, is not applicable for Mach numbers near 1.0 and may be applied only approximately for wings with round leading edges. It appears, therefore, that for unswept wings in the low supersonic range, the attainment of generally accurate flutter results from the modified strip analysis will require the use of measured

steady-state aerodynamic parameters, particularly when the local aerodynamic centers lie close to local centers of gravity.

Simplified steady-state method.- Supersonic flutter speeds calculated for wing 2001 by the simplified steady-state method with rigid-body modes are essentially coincident with corresponding results of the modified strip analysis (fig. 9) because flutter reduced frequencies for this wing were very low (less than 0.06). Since flutter results from the simplified steady-state method and from the modified strip analysis approach each other as the flutter reduced frequency approaches zero, all the supersonic results obtained for wing 2001 by this simplified steady-state method are considered to be indicative of the approximate flutter-speed and flutter-frequency levels that would be predicted by corresponding modified-strip-analysis calculations.

Both flutter speeds and frequencies calculated for this wing by the simplified steady-state method with natural vibration modes and with aerodynamic parameters obtained from shock-expansion theory (fig. 10) are in generally satisfactory agreement with experiment over the Mach number range covered ( $1.30 \leq M \leq 6.86$ ). Similar calculations employing linear-theory aerodynamic parameters yield flutter speeds that agree well with experiment at Mach numbers near 1.1 but rapidly deviate unconservatively from experimental values as Mach number increases.

Modified two-dimensional loading.- Supersonic flutter speeds calculated for wings 400, 400R, and 400L (figs. 5, 6, and 8) by use of modified two-dimensional loading are generally in good agreement with experiment. For wing 400, however, the calculations predict a hump in the flutter-speed curves near  $M = 1.1$  which is not confirmed by experiment. A similar transonic hump was indicated by the calculations of reference 46 which employed two-dimensional loading without modification for finite span. The hump for wing 400 (fig. 5) and a similar one for wing 400L (fig. 8), however, are less prominent when a small amount of structural damping is included in the calculations. Except at the lowest supersonic Mach number ( $M = 1.05$ ), the inclusion of structural damping increased the calculated flutter speeds as it did in the calculations of reference 48. The latter calculations, however, employed the theory of reference 49 which was expressed only for rigid-body motion.

Calculations for wing 400 based on two-dimensional loading coefficients without modification for finite span (fig. 5) show that the finite-span modification can be either stabilizing or destabilizing depending, for example, on Mach number.

Flutter speeds for wing 7001 calculated with modified two-dimensional loading (fig. 7) are excessively conservative and are not significantly improved by the inclusion of structural damping. This result is surprising because, of the present five wings, wing 7001 would be expected to experience aerodynamic loadings most closely representable by coefficients for two-dimensional flow. Indeed, figure 7(a) shows that the effect of the finite-span modification is relatively small for this wing, particularly in the supersonic range. It is noted, however, that the flutter calculations which employ modified two-dimensional loading also produced a second flutter boundary which is as unconservative as the previously mentioned lower boundary is conservative. For wing 7001, calculations with

unmodified two-dimensional loading produced flutter speeds which decrease as Mach number increases in the low supersonic range. Although this trend is contrary to experiment, it agrees qualitatively with the results of similar calculations for the nearly identical wing of reference 50.

Flutter speeds calculated by use of modified two-dimensional loading for wing 2001 with rigid-body vibration modes (fig. 9) behave in a manner similar to that shown by modified-strip-analysis results. That is, flutter speeds calculated from the linearized theory rise sharply and unconservatively as Mach number increases. When the linear-theory loadings are modified on the basis of shock-expansion theory, the resulting calculated flutter speeds show much better agreement with the experimental trend although the flutter-speed curve remains at a somewhat unconservative level. The latter type of calculation was not repeated with the natural vibrations modes. Such a calculation, however, would be expected to predict more accurate flutter speeds on the basis of corresponding calculations by the simplified steady-state method (fig. 10).

For all five wings, supersonic flutter frequencies calculated with modified two-dimensional loading are excessively high. (See figs. 5 to 9.)

Rectangular-wing theory.- Flutter speeds for wing 7001 calculated from rectangular-wing theory (fig. 7) are slightly conservative and appear to represent accurately the experimental trend. Similar calculations for wing 4001 yield somewhat unconservative results (fig. 8). These curves as well as the corresponding curves calculated by modified strip analysis with linear-theory aerodynamic parameters rise quite steeply with increasing Mach number. Thus, even though the curves calculated by these two methods are generally separated by a difference in Mach number of only about 0.1, the flutter speeds predicted for a given wing at a particular Mach number differ appreciably. It may be noted for wing 4001 that in the range  $1.3 \leq M \leq 1.4$ , flutter speeds obtained from rectangular-wing theory are comparable to values given by the modified strip analysis with aerodynamic parameters based on shock-expansion theory (fig. 8). Moreover, flutter frequencies for these two wings obtained by use of rectangular-wing theory compare favorably with experimental values and with values given by the modified strip analysis (figs. 7(b) and 8(b)).

For wing 2001, supersonic flutter speeds calculated from rectangular-wing theory (fig. 9) rise rapidly and unconservatively as Mach number increases. At all Mach numbers covered, these calculated flutter speeds lie between values given by modified two-dimensional loading and by modified strip analysis with linear-theory aerodynamic parameters. Except for Mach numbers close to 1.0, it appears that none of the flutter analyses which are based on linearized aerodynamic theory correctly predict either flutter-speed levels or trends for wing 2001.

Aerodynamic influence coefficients.- As expected, flutter speeds calculated for wing 4001 by the aerodynamic-influence-coefficient method (fig. 8) are nearly the same as corresponding values given by the rectangular-wing theory. However, in comparison with results from the modified strip analysis and from the rectangular-wing theory, flutter frequencies given by the aerodynamic-influence-coefficient method (fig. 8(b)) are higher and farther from the experimental values.

Quasi-steady second-order theory.- Over the Mach number range covered, flutter speeds calculated for wing 2001 from quasi-steady second-order theory with either rigid-body vibration modes or natural modes are only slightly below corresponding values given by the simplified steady-state method (figs. 9 and 10). However, when natural modes (rather than rigid-body modes) are used, the flutter-speed and flutter-frequency results of both methods are lower and in much better agreement with experimental values (fig. 10).

## DISCUSSION OF DIVERGENCE RESULTS

### Subsonic Speed Range

Modified strip analysis and modified two-dimensional loading.- As indicated previously, when the reduced frequency is zero, the equations of the modified strip analysis are identical to those of the simplified steady-state method. Furthermore, the expressions for divergence obtained from the modified strip analysis and from modified two-dimensional loading are identical so that all three methods predict the same divergence speeds. Figures 5 to 9 show that as Mach number increases, the subsonic divergence speeds obtained by use of linear-theory aerodynamic parameters in these methods characteristically decrease at a more rapid rate than do the corresponding calculated flutter speeds. Although only flutter was encountered experimentally, the calculated subsonic divergence-speed curves for wings 400, 400R, 7001, and 4001 drop below the experimental flutter points and below the calculated flutter boundaries at Mach numbers near 1.0. Thus these predicted divergence speeds are obviously conservative, at least at the higher subsonic Mach numbers.

Subsonic kernel function.- The subsonic kernel-function method was employed in divergence calculations only for wing 2001 (fig. 9). Throughout the subsonic range the resulting divergence speeds agree closely with those given by the modified strip analysis and by modified two-dimensional loading, although experimental confirmation of the calculated values is not available.

### Supersonic Speed Range

Modified strip analysis and modified two-dimensional loading.- All the supersonic divergence speeds calculated from the modified strip analysis and from modified two-dimensional loading lie well above all calculated flutter boundaries. (See figs. 5, 6, and 8.) These divergence curves rise very steeply with increasing Mach number, and all become infinite at relatively low supersonic Mach numbers. In fact, supersonic divergence calculations for wing 7001 did not indicate any finite divergence speeds in the Mach number range covered. Calculations for wing 2001 (figs. 9 and 10) did not yield finite divergence speeds for Mach numbers above 1.30.

Rectangular-wing theory.- The divergence speed for wing 4001 at  $M = 2/\sqrt{3}$  has been calculated from rectangular-wing theory. The resulting divergence speed (fig. 8(a)) is only about 6 percent above the corresponding calculated flutter

speed and is also close to the flutter speed predicted by the aerodynamic-influence-coefficient method.

## SUMMARY OF RESULTS

Subsonic and supersonic flutter and divergence calculations have been made for five unswept wings by several analytical methods. The results have been compared with experimental flutter data in order to assess the usefulness of each method for predicting aeroelastic instabilities, particularly near sonic speed and in the hypersonic range.

For Mach numbers below about 0.75, little difference appeared between flutter speeds predicted by modified strip analysis, by two-dimensional loading modified to account for the finite planform, and by subsonic kernel function. All calculated flutter boundaries appeared to be at reasonable levels. A simplified steady-state method, which represents the zero-frequency limiting case of the modified strip analysis, gave similar results for a wing which fluttered at low reduced frequencies.

This investigation, together with previously published related information, indicates that the modified strip analysis, which has previously been shown to yield accurate transonic flutter results for swept wings, may be expected to yield generally accurate subsonic flutter results for unswept wings only up to a Mach number of about 0.85 because of limitations inherent in the method. At these higher subsonic Mach numbers, results obtained with modified two-dimensional loading were not consistently satisfactory. The subsonic-kernel-function method yielded accurate flutter results up to Mach numbers above 0.90. For the wing which fluttered at low reduced frequencies, the simplified steady-state method gave flutter speeds which were very close to those from the subsonic kernel function.

Results of the modified strip analysis become sensitive to small changes in local-aerodynamic-center position when the aerodynamic centers lie close to local centers of gravity. Under these conditions, which frequently occur for unswept wings even at relatively low supersonic Mach numbers, linearized aerodynamic theory is not adequate, and satisfactory flutter prediction by the modified strip analysis requires that the aerodynamic centers be located by the more accurate nonlinear theories, which account for effects of finite wing thickness, or by steady-flow experiments. Modified two-dimensional loading yielded accurate flutter boundaries for some wings in the low supersonic range, but, as in the subsonic range, the results were not consistently satisfactory. Rectangular-wing theory, which is based on linearized aerodynamic theory, gave reasonable flutter results at low supersonic Mach numbers, and, as expected, these flutter boundaries were closely approximated by the aerodynamic-influence-coefficient method. For the wing which fluttered at low reduced frequencies, all calculations employing linearized aerodynamic theory yielded flutter speeds that quickly became excessively unconservative as Mach number increased. These calculations included the modified strip analysis, the simplified steady-state method, modified two-dimensional loading, and rectangular-wing theory. On the other hand, when

shock-expansion theory was employed in the modified strip analysis, in the simplified steady-state method, and in modified two-dimensional loading, all three methods were indicated to be capable of predicting satisfactory flutter boundaries for this wing even into the hypersonic range. Satisfactory results were also obtained with quasi-steady second-order theory.

Subsonic divergence speeds calculated from the modified strip analysis were coincident with those obtained with modified two-dimensional loading and were very close to those given by the subsonic kernel function. Although no experimental divergence data were available for comparison, the calculated divergence boundaries were indicated to be conservative in the high subsonic range because they were below experimental flutter points.

Calculated supersonic divergence boundaries were generally well above corresponding flutter boundaries and rose very steeply as Mach number increased.

Langley Research Center,  
National Aeronautics and Space Administration,  
Langley Station, Hampton, Va., October 4, 1963.

## REFERENCES

1. Yates, E. Carson, Jr.: Calculation of Flutter Characteristics for Finite-Span Swept or Unswept Wings at Subsonic and Supersonic Speeds by a Modified Strip Analysis. NACA RM L57L10, 1958.
2. Yates, E. Carson, Jr.: Some Effects of Variations in Density and Aerodynamic Parameters on the Calculated Flutter Characteristics of Finite-Span Swept and Unswept Wings at Subsonic and Supersonic Speeds. NASA TM X-182, 1960.
3. Yates, E. Carson, Jr., and Bennett, Robert M.: Use of Aerodynamic Parameters from Nonlinear Theory in Modified-Strip-Analysis Flutter Calculations for Finite-Span Wings at Supersonic Speeds. NASA TN D-1824, 1963.
4. Yates, E. Carson, Jr.: Use of Experimental Steady-Flow Aerodynamic Parameters in the Calculation of Flutter Characteristics for Finite-Span Swept or Unswept Wings at Subsonic, Transonic, and Supersonic Speeds. NASA TM X-183, 1960.
5. Pines, Samuel: An Elementary Explanation of the Flutter Mechanism. Proc. Nat. Specialists Meeting on Dynamics and Aeroelasticity (Fort Worth, Texas), Inst. Aero. Sci., Nov. 1958, pp. 52-58.
6. MacNeal, Richard H.: Simple Analytical Solutions of the Binary Flutter Problem. WADD Tech. Note 60-130, U.S. Air Force, Mar. 1960.
7. Zimmerman, Norman H.: Elementary Static Aerodynamics Adds Significance and Scope in Flutter Analyses. Structural Dynamics of High Speed Flight, ACR-62, vol. 1, Office of Naval Res., Apr. 1961, pp. 28-84.
8. Mazelsky, Bernard, and Amey, Harry B., Jr.: Basic Principles of the Indicial Lifting-Surface Flutter-Analysis Procedure. ASD-TDR-62-44, U.S. Air Force, May 1962.
9. Garrick, I. E., and Rubinow, S. I.: Flutter and Oscillating Air-Force Calculations for an Airfoil in a Two-Dimensional Supersonic Flow. NACA Rep. 846, 1946. (Supersedes NACA TN 1158.)
10. Jordan, P. F.: Aerodynamic Flutter Coefficients for Subsonic, Sonic, and Supersonic Flow (Linear Two-Dimensional Theory). R. & M. No. 2932, British A.R.C., 1957.
11. Watkins, Charles E., Runyan, Harry L., and Woolston, Donald S.: On the Kernel Function of the Integral Equation Relating the Lift and Downwash Distributions of Oscillating Finite Wings in Subsonic Flow. NACA Rep. 1234, 1955. (Supersedes NACA TN 3131.)
12. Watkins, Charles E., Woolston, Donald S., and Cunningham, Herbert J.: A Systematic Kernel Function Procedure for Determining Aerodynamic Forces on Oscillating or Steady Finite Wings at Subsonic Speeds. NASA TR R-48, 1959.

13. Miles, John W.: A General Solution for the Rectangular Airfoil in Supersonic Flow. Quarterly Appl. Math., vol. XI, no. 1, Apr. 1953, pp. 1-8.
14. Brandstatter, J., and Mortzschky, H.: A Method for Calculating the Potential on a Tapered Oscillating Wing in Supersonic Flow. Mathematical Analysis Dept. Memo. No. 245, Lockheed Aircraft Corp., Apr. 1, 1954.
15. Mortzschky, H., and Brandstatter, J.: Calculations of the Potential on a Tapered Wing Oscillating in a Supersonic Flow Field. Mathematical Analysis Dept. Memo. No. 246, Lockheed Aircraft Corp., Oct. 15, 1954.
16. Mortzschky, H. A.: Calculation of Pressure Coefficients for a Tapered Wing With Constant Downwash. Mathematical Analysis Dept. Study No. 38, Lockheed Aircraft Corp., May 17, 1955. (Available from ASTIA as AD 121568.)
17. Lessing, Henry C., Troutman, John L., and Menees, Gene P.: Experimental Determination of the Pressure Distribution on a Rectangular Wing Oscillating in the First Bending Mode for Mach Numbers From 0.24 to 1.30. NASA TN D-344, 1960.
18. Bond, Reuben, Packard, Barbara B., Warner, Robert W., and Summers, Audrey L.: A Method for Calculating the Generalized Aerodynamic Forces on Rectangular Wings Deforming Symmetrically in Supersonic Flight With Indicial or Sinusoidal Time Dependence. NASA TN D-1206, 1962.
19. Pines, S., and Dugundji, J.: Aerodynamic Flutter Derivatives of a Flexible Wing With Supersonic Edges. ATC Rep. No. ARTC-7, Aircraft Industries Assoc. (Washington, D.C.), Feb. 15, 1954.
20. Pines, Samuel, Dugundji, John, and Neuringer, Joseph: Aerodynamic Flutter Derivatives for a Flexible Wing With Supersonic and Subsonic Edges. Jour. Aero. Sci., vol. 22, no. 10, Oct. 1955, pp. 693-700.
21. Pines, S., and Dugundji, J.: Application of Aerodynamic Flutter Derivatives to Flexible Wings With Supersonic and Subsonic Edges. Rep. No. E-SAF-2, Republic Aviation Corp., Apr. 15, 1954.
22. Li, Ta: Aerodynamic Influence Coefficients for an Oscillating Finite Thin Wing in Supersonic Flow. Jour. Aero. Sci., vol. 23, no. 7, July 1956, pp. 613-622.
23. Zartarian, Garabed, and Hsu, Pao-Tan: Theoretical Studies on the Prediction of Unsteady Supersonic Airloads on Elastic Wings. WADC Tech. Rep. 56-97, Pts. I and II, U.S. Air Force.  
Part I. Investigations on the Use of Oscillatory Supersonic Aerodynamic Influence Coefficients. ASTIA Doc. No. AD 110591, Dec. 1955.  
Part 2. Rules for Application of Oscillatory Supersonic Aerodynamic Influence Coefficients. ASTIA Doc. No. AD 110592, Feb. 1956.
24. Van Dyke, Milton D.: A Study of Second-Order Supersonic Flow Theory. NACA Rep. 1081, 1952. (Supersedes NACA TN 2200.)



25. Morgan, Homer G., Huckel, Vera, and Runyan, Harry L.: Procedure for Calculating Flutter at High Supersonic Speed Including Camber Deflections, and Comparison With Experimental Results. NACA TN 4335, 1958.
26. Bennett, Robert M., and Yates, E. Carson, Jr.: A Study of Several Factors Affecting the Flutter Characteristics Calculated for Two Swept Wings by Piston Theory and by Quasi-Steady Second-Order Theory and Comparison With Experiments. NASA TN D-1794, 1963.
27. Van Dyke, Milton D.: Supersonic Flow Past Oscillating Airfoils Including Nonlinear Thickness Effects. NACA Rep. 1183, 1954. (Supersedes NACA TN 2982.)
28. Runyan, Harry L., and Morgan, Homer G.: Flutter at Very High Speeds. NASA TN D-942, 1961. (Supersedes NACA RM L57D16a.)
29. Lighthill, M. J.: Oscillating Airfoils at High Mach Number. Jour. Aero. Sci., vol. 20, no. 6, June 1953, pp. 402-406.
30. Ashley, Holt, and Zartarian, Garabed: Piston Theory - A New Aerodynamic Tool for the Aeroelastician. Jour. Aero. Sci., vol. 23, no. 12, Dec. 1956, pp. 1109-1118.
31. Chawla, Jagannath P.: Aeroelastic Instability at High Mach Number. Jour. Aero. Sci., vol. 25, no. 4, Apr. 1958, pp. 246-258.
32. Landahl, Marten T.: The Flow Around Oscillating Low Aspect Ratio Wings at Transonic Speeds. KTH Aero TN 40, Div. Aero., Roy. Inst. Tech. (Stockholm), 1954.
33. Landahl, Marten T.: Theoretical Studies of Unsteady Transonic Flow - Part I. Linearization of the Equations of Motion. FFA Rep. 77, Aero. Res. Inst. of Sweden (Stockholm), 1958.
34. Landahl, Marten T.: Theoretical Studies of Unsteady Transonic Flow - Part IV. The Oscillating Rectangular Wing With Control Surface. FFA Rep. 80, Aero. Res. Inst. of Sweden (Stockholm), 1959.
35. Davies, D. E.: Three-Dimensional Sonic Theory. Aerodynamic Aspects. Pt. II of AGARD Manual on Aeroelasticity, ch. 4, W. P. Jones, ed., North Atlantic Treaty Organization (Paris).
36. Unangst, John R., and Jones, George W., Jr.: Some Effects of Sweep and Aspect Ratio on the Transonic Flutter Characteristics of a Series of Thin Cantilever Wings Having a Taper Ratio of 0.6. NASA TN D-1594, 1963. (Supersedes NACA RM L55I13a and NACA RM L53G10a.)
37. Bursnall, William J.: Initial Flutter Tests in the Langley Transonic Blow-down Tunnel and Comparison With Free-Flight Flutter Results. NACA RM L52K14, 1953.

38. Pratt, George L.: Experimental Flutter Investigation of a Thin Unswept Wing at Transonic Speeds. NACA RM L55A18, 1955.
39. Hanson, Perry W.: Aerodynamic Effects of Some Configuration Variables on the Aeroelastic Characteristics of Lifting Surfaces at Mach Numbers From 0.7 to 6.86. NASA TN D-984, 1961.
40. Unangst, John R.: Transonic Flutter Characteristics of an Aspect-Ratio-4, 45° Sweptback, Taper-Ratio-0.2 Planform. NASA TM X-136, 1959.
41. Yates, E. Carson, Jr., Land, Norman S., and Foughner, Jerome T., Jr.: Measured and Calculated Subsonic and Transonic Flutter Characteristics of a 45° Sweptback Wing Planform in Air and in Freon-12 in the Langley Transonic Dynamics Tunnel. NASA TN D-1616, 1963.
42. Yates, E. Carson, Jr.: Subsonic and Supersonic Flutter Analysis of a Highly Tapered Swept-Wing Planform, Including Effects of Density Variation and Finite Wing Thickness, and Comparison With Flutter Experiments. NASA TM X-764, 1963.
43. Von Doenhoff, Albert E., Braslow, Albert L., and Schwartzberg, Milton A.: Studies of the Use of Freon-12 as a Wind-Tunnel Testing Medium. NACA TN 3000, 1953.
44. Falkner, V. M.: The Calculation of Aerodynamic Loading on Surfaces of Any Shape. R. & M. No. 1910, British A.R.C., Aug. 1943.
45. Lagerstrom, P. A., Wall, D., and Graham, M. E.: Formulas in Three-Dimensional Wing Theory. Rep. No. SM-11901, Douglas Aircraft Co., Inc., July 8, 1946.
46. Young, J. P.: Dyna-Soar Step I Cantilevered Fin Flutter Report. Tech. Note DS 112-61 (Contract No. AF04(647)-610), The Martin Co., Dec. 1, 1961.
47. Cooley, Dale E.: Theoretical Studies of the Effects of Structural Damping on Flutter at Hypersonic Speeds. ASD Tech. Note 61-91, U.S. Air Force, Oct. 1961.
48. Guyett, P. R.: Supersonic Wind-Tunnel Flutter Tests of Two Rectangular Wings. R. & M. No. 3080, British A.R.C., 1958.
49. Acum, W. E. A.: Aerodynamic Forces on Rectangular Wings Oscillating in a Supersonic Air Stream. R. & M. No. 2763, British A.R.C., 1954.
50. Lauten, William T., Jr., and Nelson, Herbert C.: Results of Two Free-Fall Experiments on Flutter of Thin Unswept Wings in the Transonic Speed Range. NACA TN 3902, 1957. (Supersedes NACA RM L51C08.)

TABLE I.- WING AND DENSITY PARAMETERS EMPLOYED IN

## FLUTTER AND DIVERGENCE ANALYSES

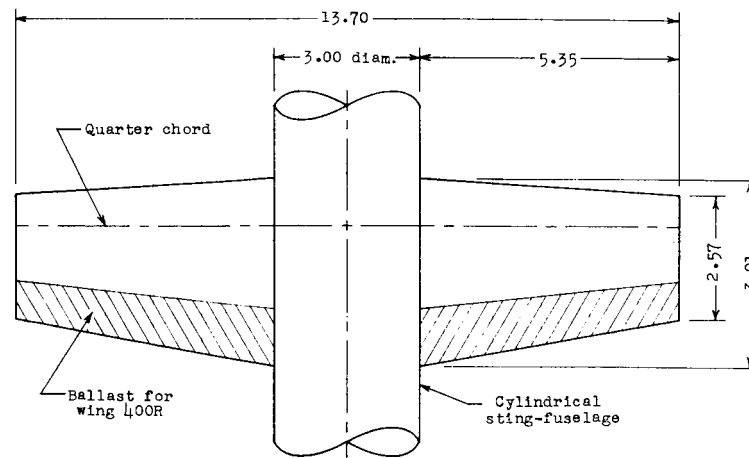
Wing	Wing geometry (a)					Thickness, percent chord	Uncoupled-mode frequencies, radians/sec			Coupled-mode frequency, radians/sec		Density parameters	
	A	A <sub>p</sub>	λ	λ <sub>p</sub>	Airfoil		ω <sub>n,1</sub>	ω <sub>n,2</sub>	ω <sub>a</sub>	ω <sub>1</sub>	ω <sub>2</sub>	ρ, slug/cu ft	μ
400	4.000	3.305	0.6	0.6576	NACA 65A004	4.0	946	4,415	2,463	-----	-----	0.002378	38.48
400R	4.000	3.305	.6	.6576	NACA 65A004	4.0	570	2,810	1,982	-----	-----	.003100	59.20
7001	7.387	6.036	1.0	1.0000	{ NACA 65A004 (root) NACA 65A002 (tip) }	{ 4.0 (root) 2.0 (tip) }	380	1,695	2,271	-----	-----	.005500	77.26
4001	4.000	3.460	1.0	1.0000			Hexagon	1.5	465	2,890	2,048	-----	-----
2001	2.000	2.000	1.0	1.0000	Diamond	9.0	{ 80.7 137.2 223.0 }	-----	251.3	{ 71.0 to 76.7 126 to 128 197 to 204 }	{ 258 to 270 415 to 421 634 to 650 }	Varies (See ref. 39)	Varies (See ref. 39)
								-----	427.0				
								-----	694.0				

<sup>a</sup>The quarter-chord sweep angle is zero for all wings.

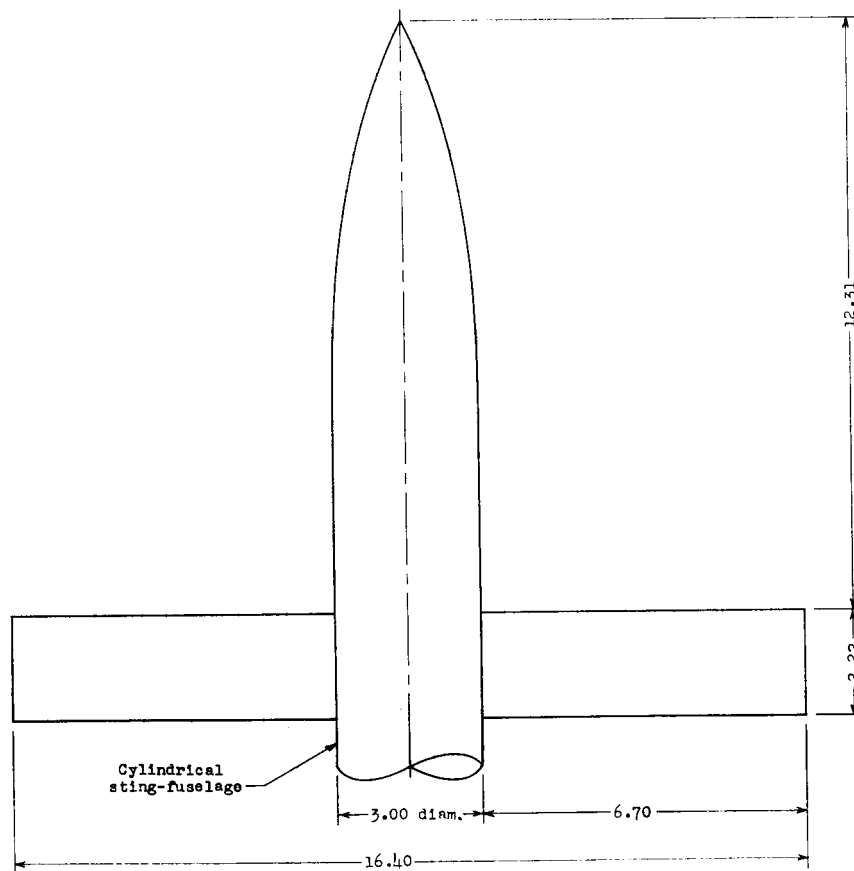
TABLE II.- SUMMARY OF FLUTTER AND DIVERGENCE CALCULATIONS

Analyses					Mach numbers				
Type	Source of aerodynamic parameters	Effect of finite span included	References	Wing 400	Wing 400R	Wing 7001	Wing 4001	Wing 2001	
Modified strip analysis	Linearized theory	Approximately	1, 2	<sup>a</sup> (0 to $\sqrt{2}$ )	<sup>a</sup> (0 to $\sqrt{2}$ )	<sup>a</sup> (0 to $\sqrt{2}$ )	<sup>a</sup> (0 to $\sqrt{2}$ )	<sup>a</sup> (0 to 3.00)	
	Shock-expansion theory	Approximately	3	-----	-----	-----	<sup>a</sup> (1.30 to $\sqrt{2}$ )	<sup>a</sup> (1.30 to 6.86)	
	Wind-tunnel test	Approximately	4	0.60 to 0.80	0.60 to 0.80	-----	-----	-----	
	Flight test	Approximately	4	1.41	1.41	-----	-----	-----	
Simplified steady-state method	Linearized theory	Approximately	5 to 7	-----	-----	-----	-----	<sup>a</sup> <sup>b</sup> (0 to 1.17)	
	Shock-expansion theory	Approximately	-----	-----	-----	-----	-----	<sup>a</sup> <sup>b</sup> (1.30 to 6.86)	
Modified two-dimensional loading	Linearized theory	No	9, 10	0 to 2.00	-----	0 to 10/7	-----	-----	
	Linearized theory	Approximately	-----	<sup>a</sup> (0 to 2.00)	<sup>a</sup> (0 to 2.00)	<sup>a</sup> (0 to 1.35)	<sup>a</sup> (0 to 10/7)	<sup>a</sup> (0 to 10/3)	
Subsonic kernel function	Shock-expansion theory	Approximately	-----	-----	-----	-----	-----	1.30 to 5.00	
	Linearized theory	Yes	11, 12	0 to 0.96	0 to 0.99	-----	-----	<sup>a</sup> <sup>b</sup> (0 to 0.99)	
Rectangular-wing theory	Linearized theory	Yes	13 to 18	-----	-----	<sup>a</sup> <sup>b</sup> (2/3 to 1.40)	<sup>a</sup> <sup>b</sup> (2/3 to 1.40)	10/7 to 3.00	
Aerodynamic influence coefficients	Linearized theory	Yes	19 to 23	-----	-----	-----	<sup>a</sup> <sup>b</sup> (2/3 to $\sqrt{2}$ )	-----	
Quasi-steady second-order theory	Second-order theory	Approximately	24 to 26	-----	-----	-----	-----	<sup>b</sup> (1.64 to 6.86)	

<sup>a</sup>Divergence calculations included.<sup>b</sup>Coupled-mode calculations included.

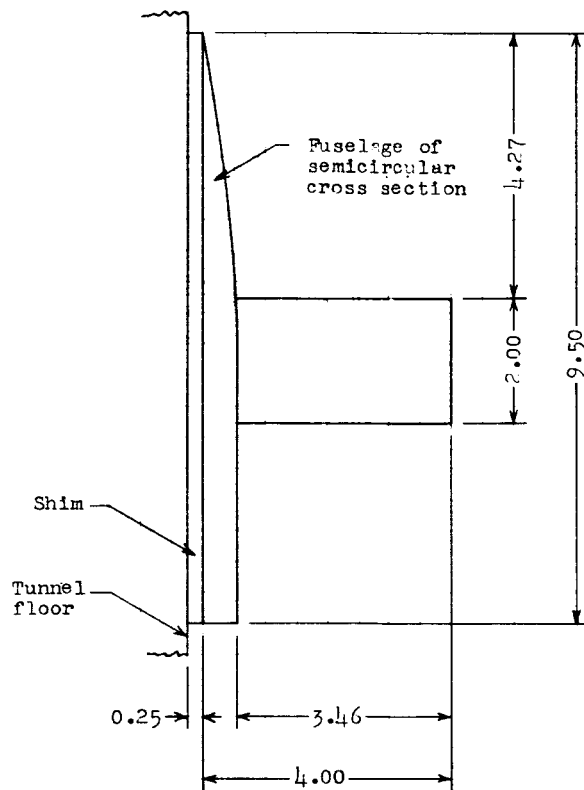


(a) Wings 400 and 400R.

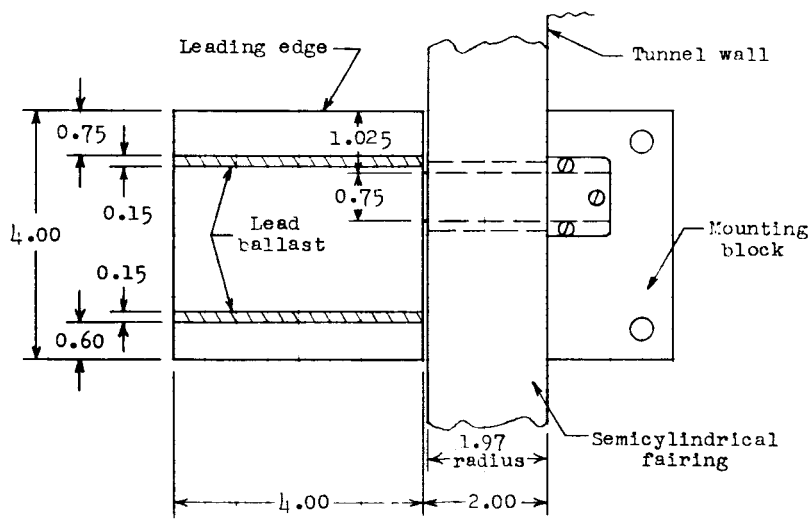


(b) Wing 7001.

Figure 1.- Wings employed in flutter analyses. All dimensions are in inches.



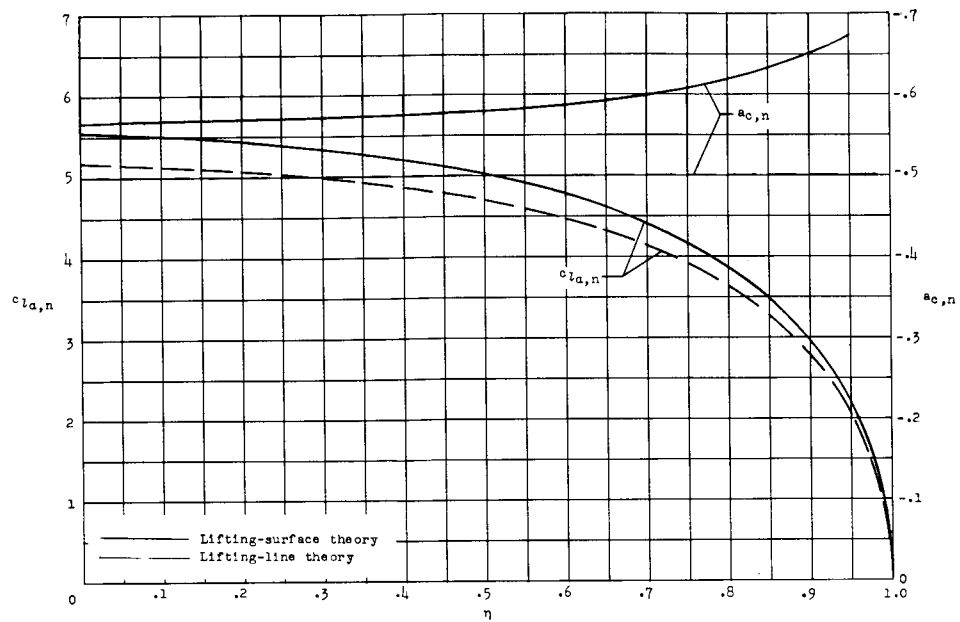
(c) Wing 4001.



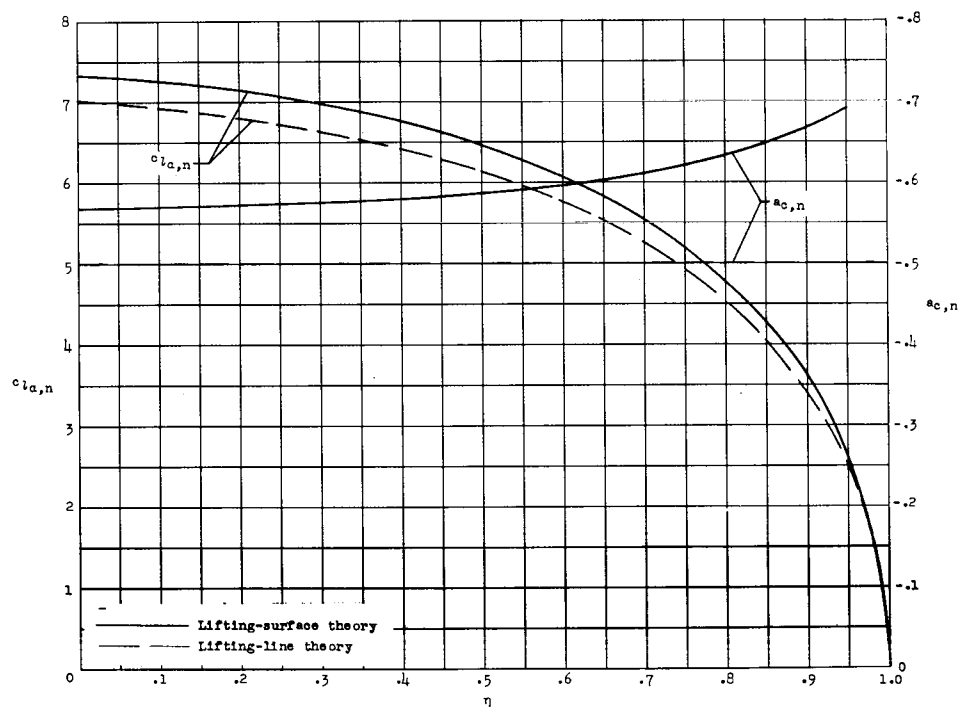
Mounting-shaft thicknesses were 0.033, 0.047, or 0.065 inch

(d) Wing 2001.

Figure 1.- Concluded.

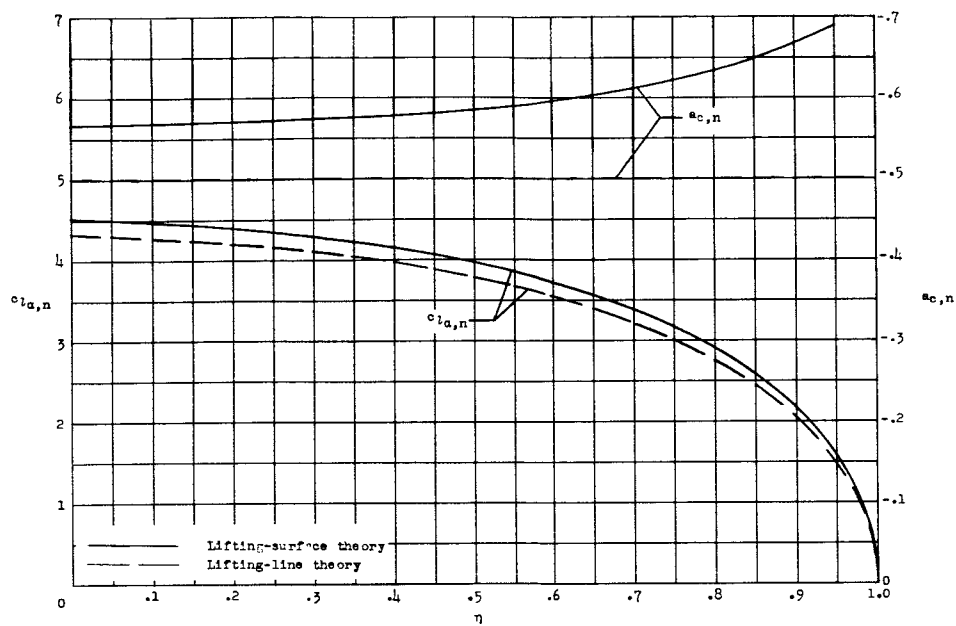


(a)  $M = 0$ .

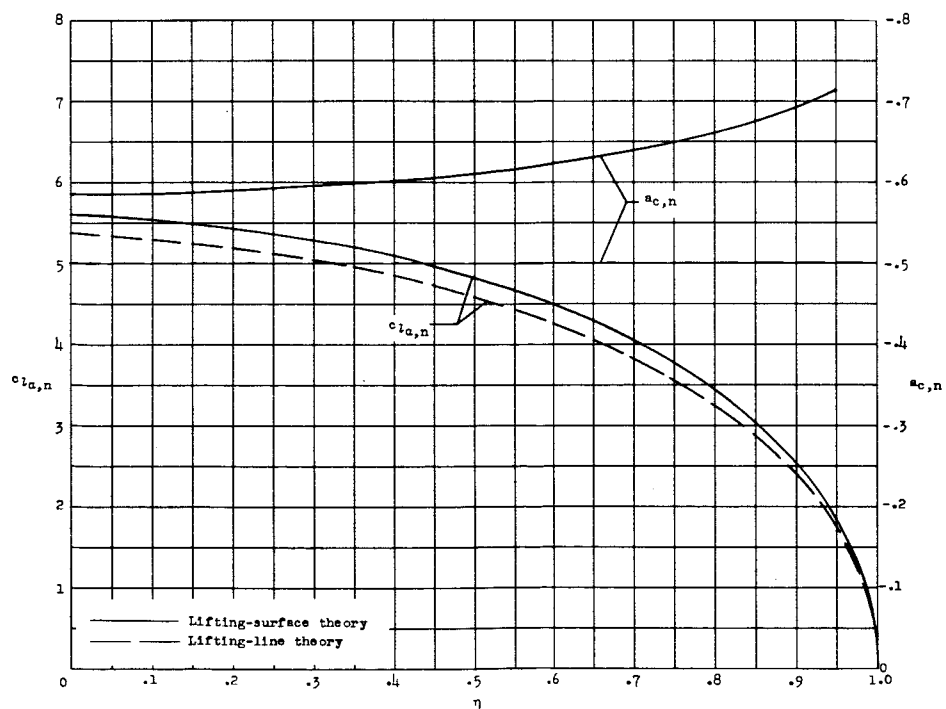


(b)  $M = 0.75$ .

Figure 2.- Spanwise distributions of steady-flow aerodynamic parameters for wing 7001.



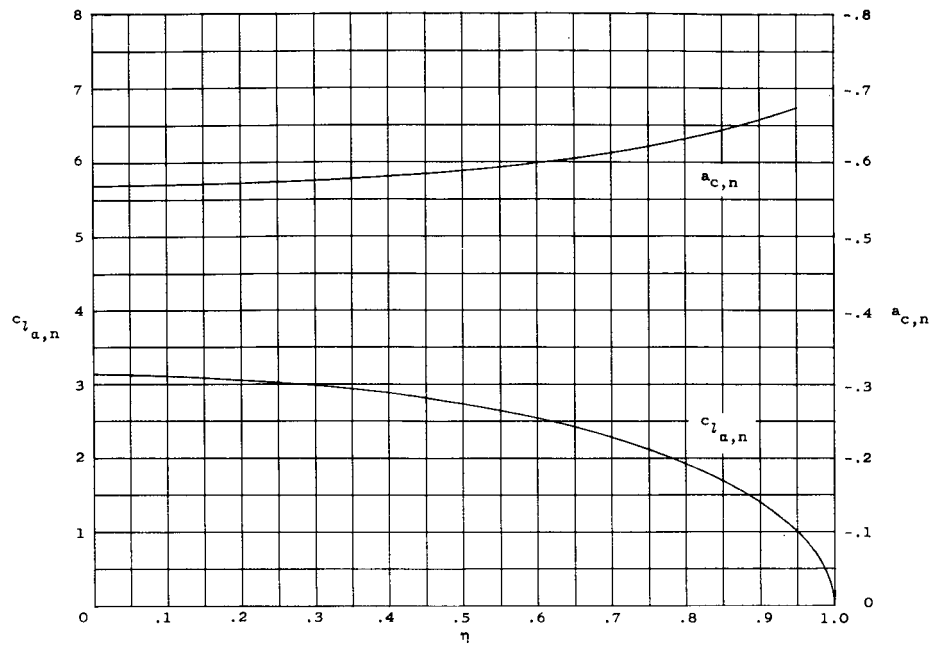
(a)  $M = 0$ .



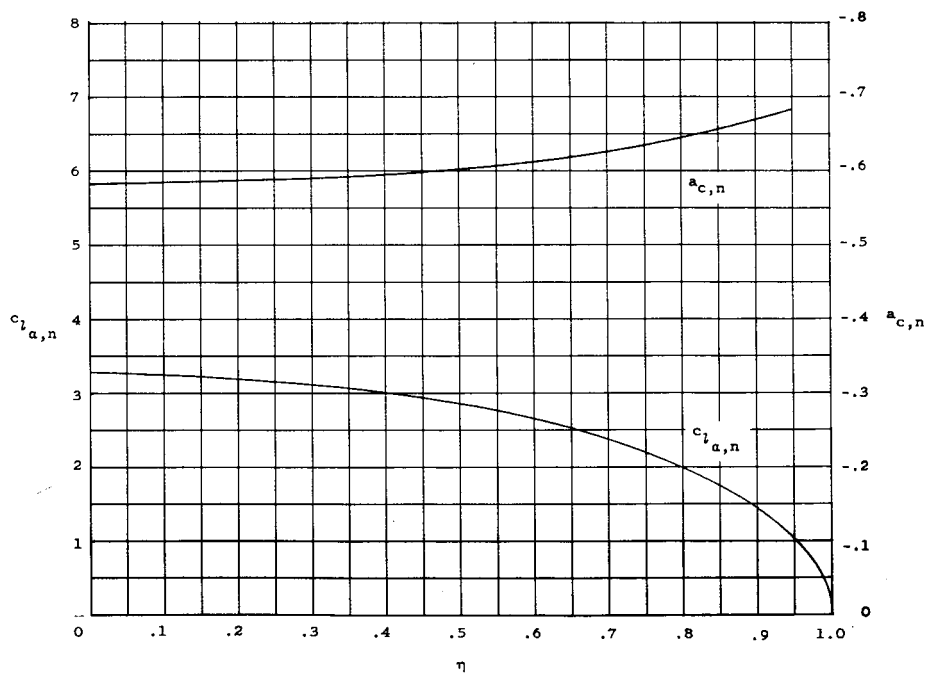
(b)  $M = 0.75$ .

Figure 3.- Spanwise distributions of steady-flow aerodynamic parameters for wing 4001.



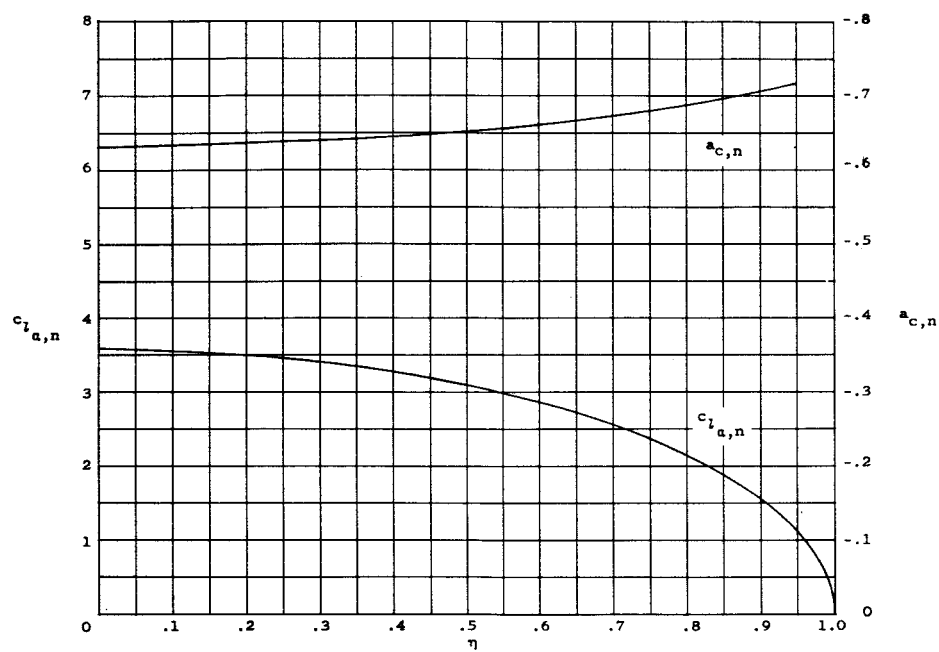


(a)  $M = 0$ ;  $e = 1.000$ .

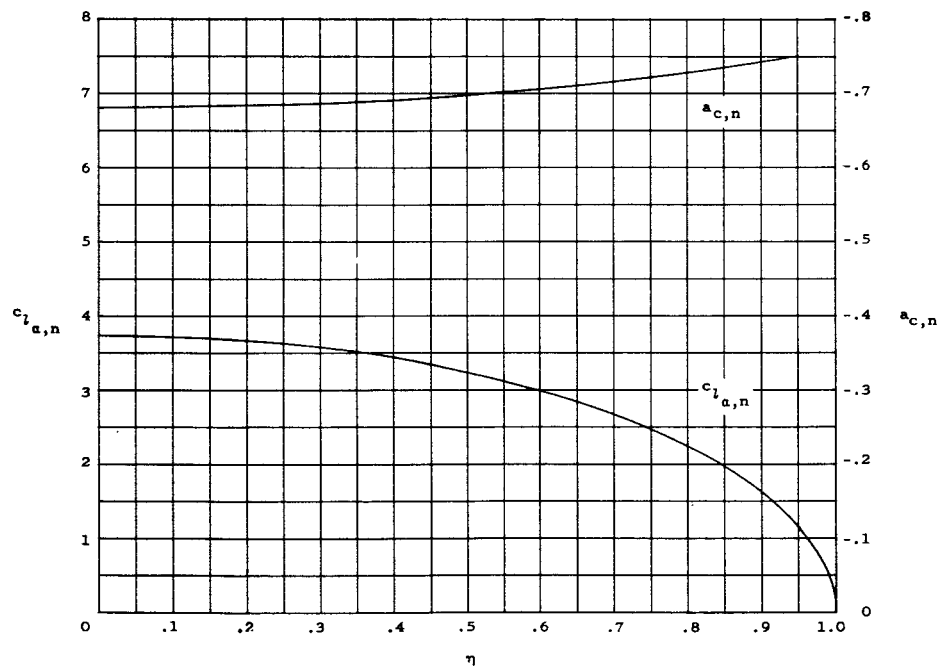


(b)  $M = 0.5$ ;  $e = 1.030$ .

Figure 4.- Spanwise distributions of steady-flow aerodynamic parameters for wing 2001 in air.

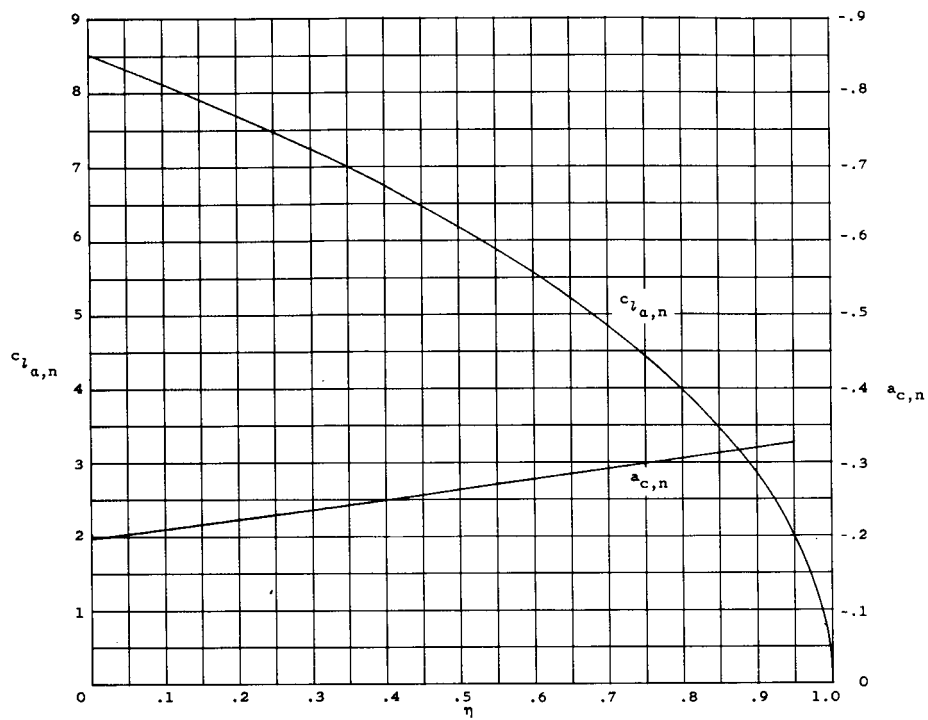


(c)  $M = 0.8$ ;  $e = 1.065$ .

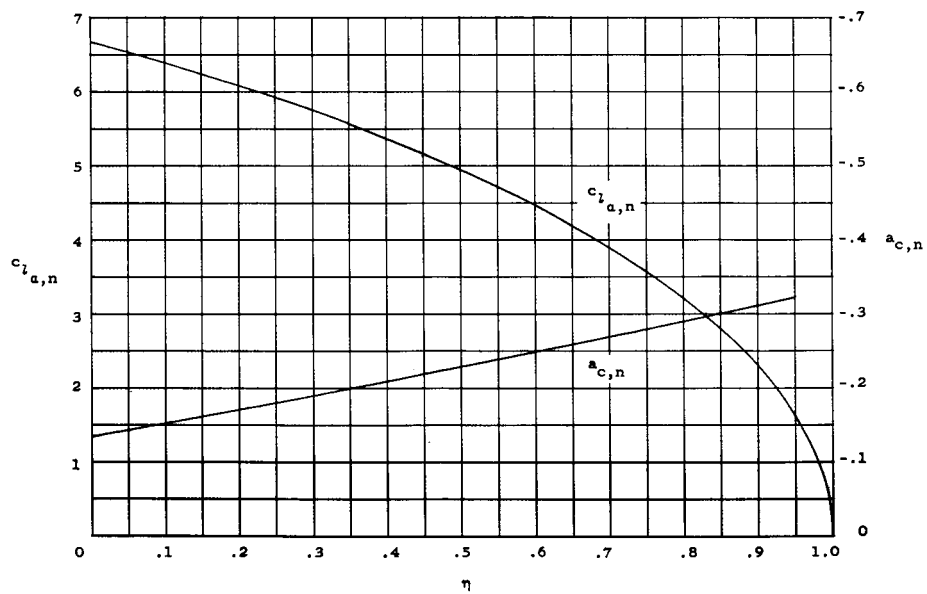


(d)  $M = 0.9$ ;  $e = 1.075$ .

Figure 4.- Continued.

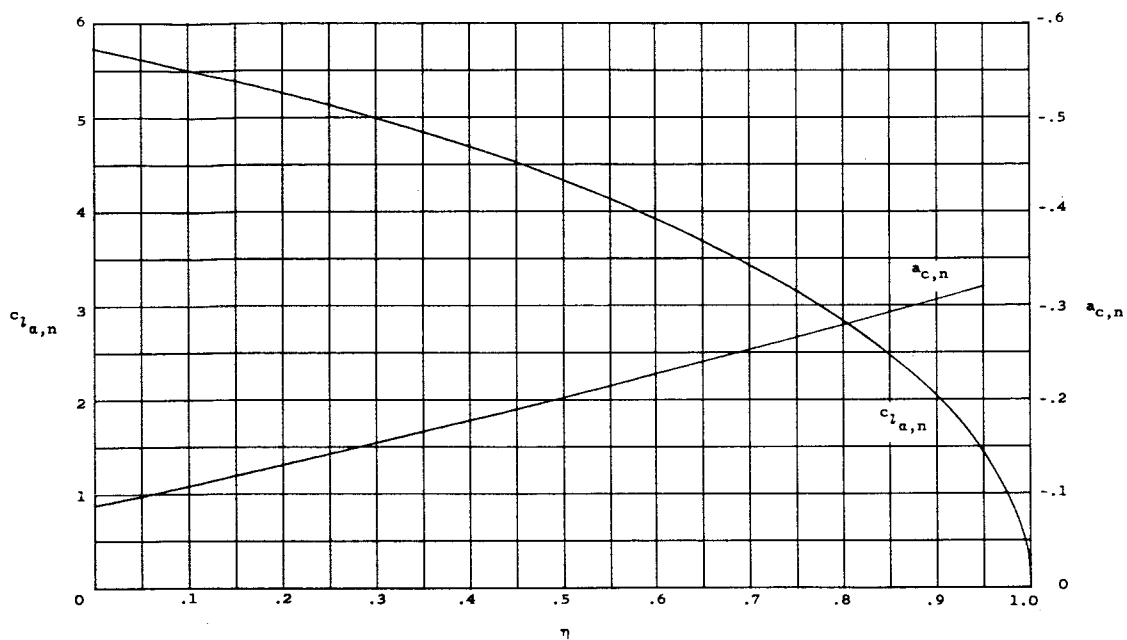


(e)  $M = 1.05$ ;  $e = 1.110$ .

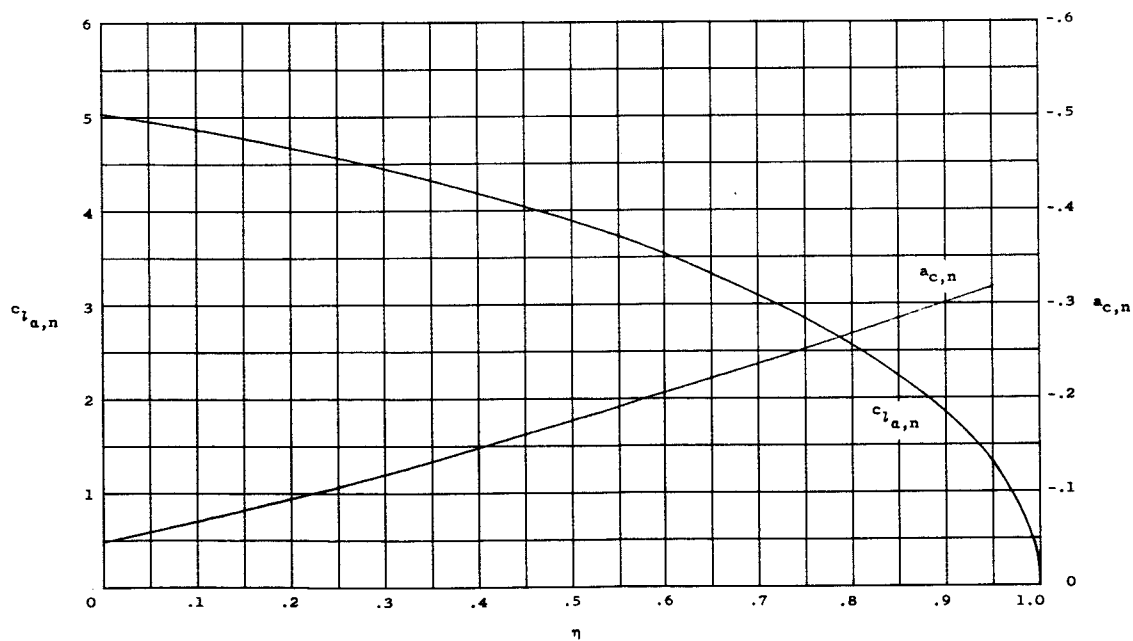


(f)  $M = 1.111$ ;  $e = 1.110$ .

Figure 4.- Continued.

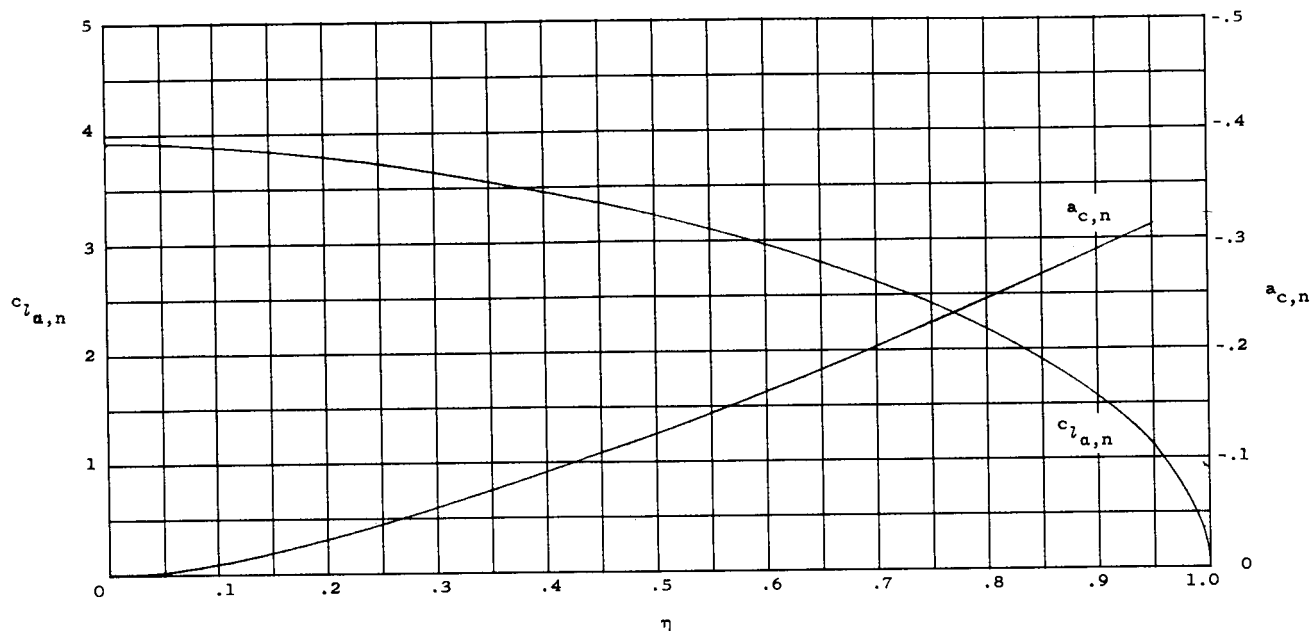


(g)  $M = 1.1765$ ;  $e = 1.110$ .

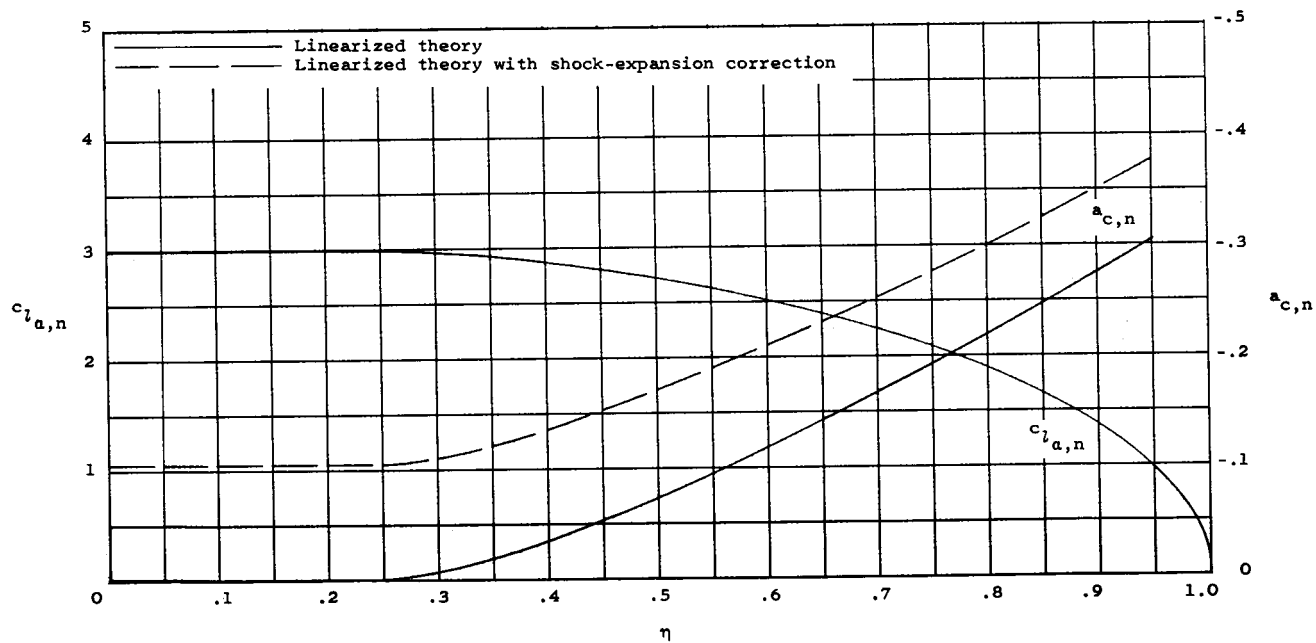


(h)  $M = 1.25$ .

Figure 4.- Continued.

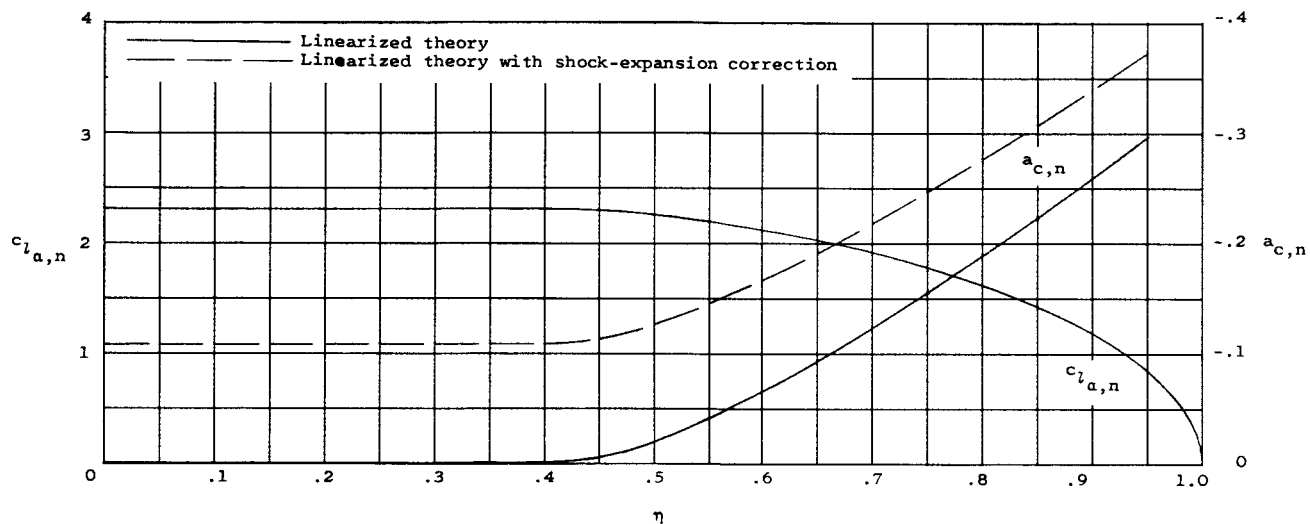


(i)  $M = 1.4286$ .

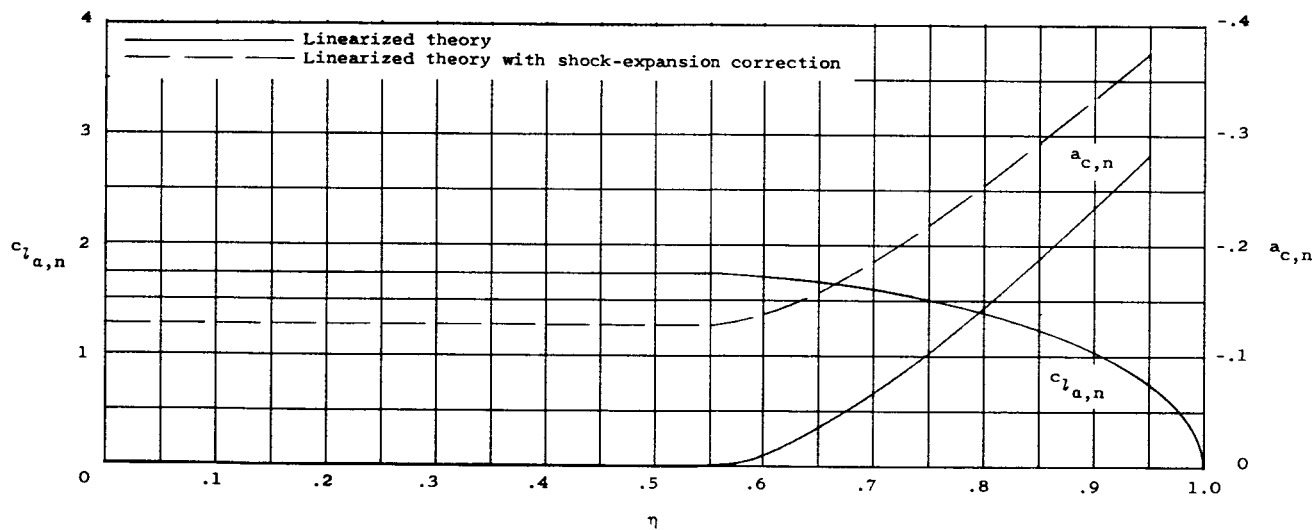


(j)  $M = 1.6667$ .

Figure 4.- Continued.

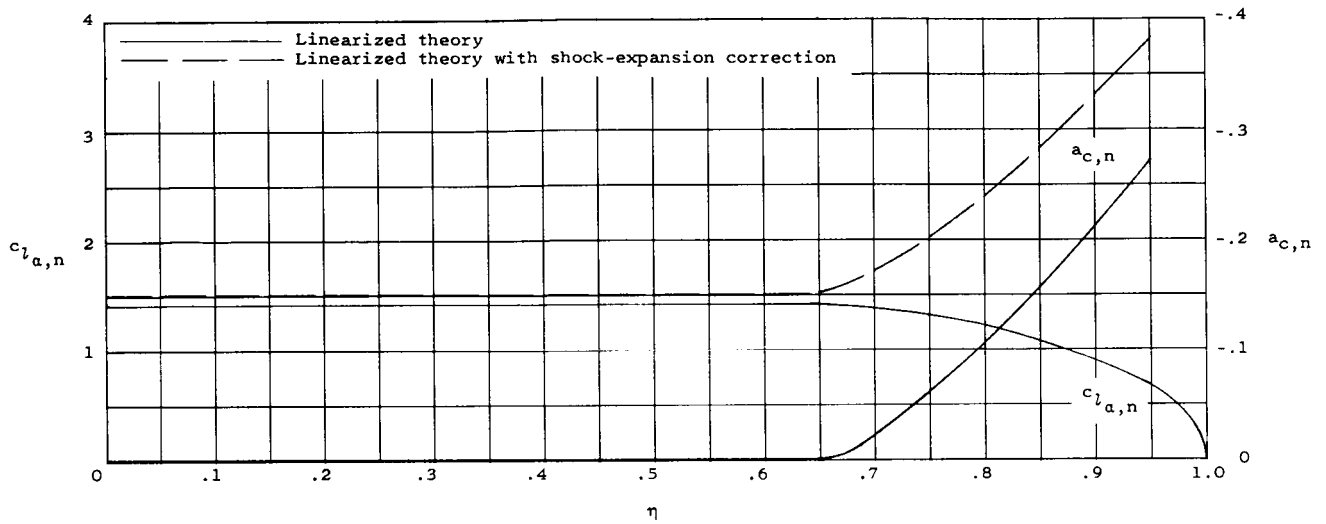


(k)  $M = 2.00$ .

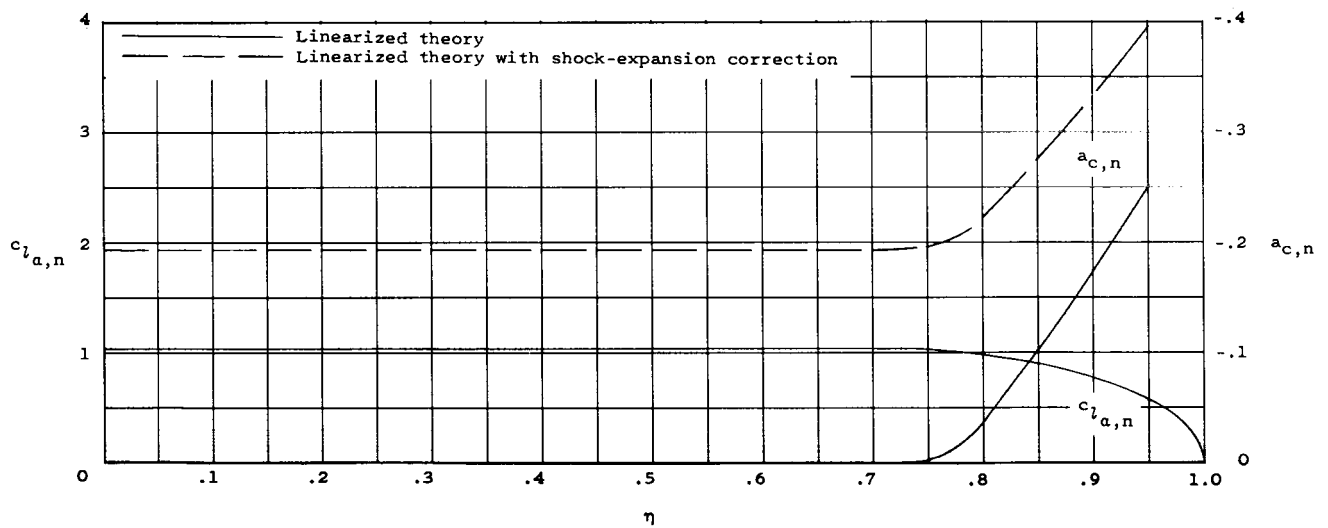


(l)  $M = 2.50$ .

Figure 4.- Continued.

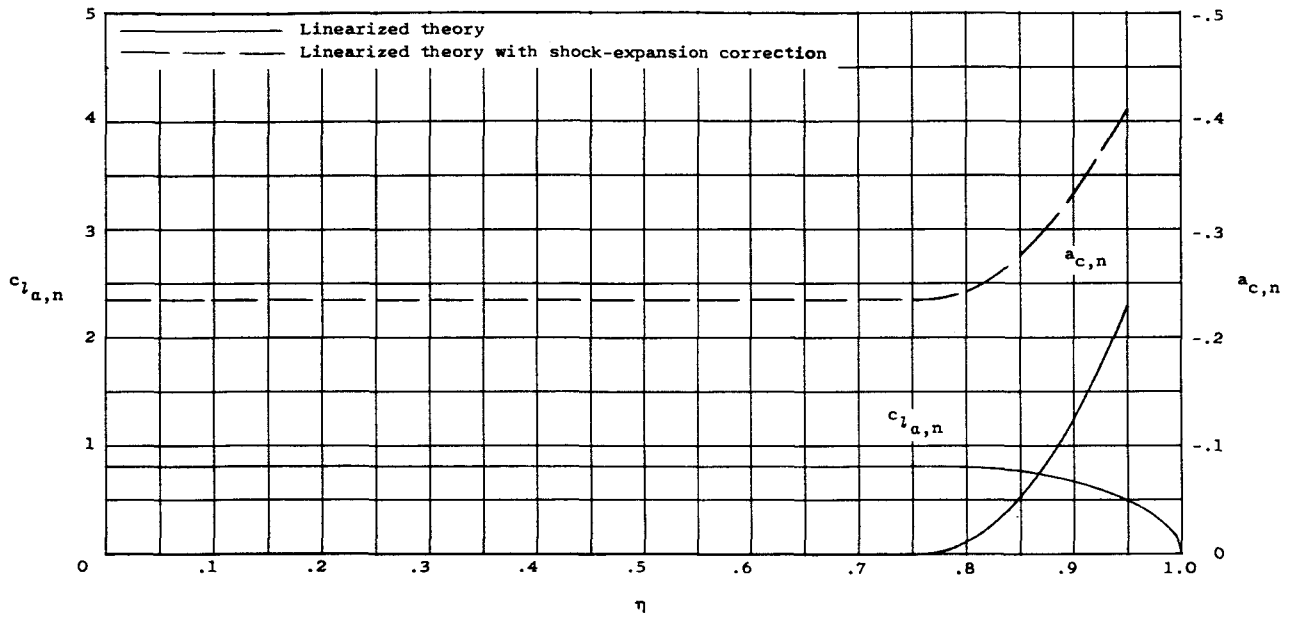


(m)  $M = 3.00$ .

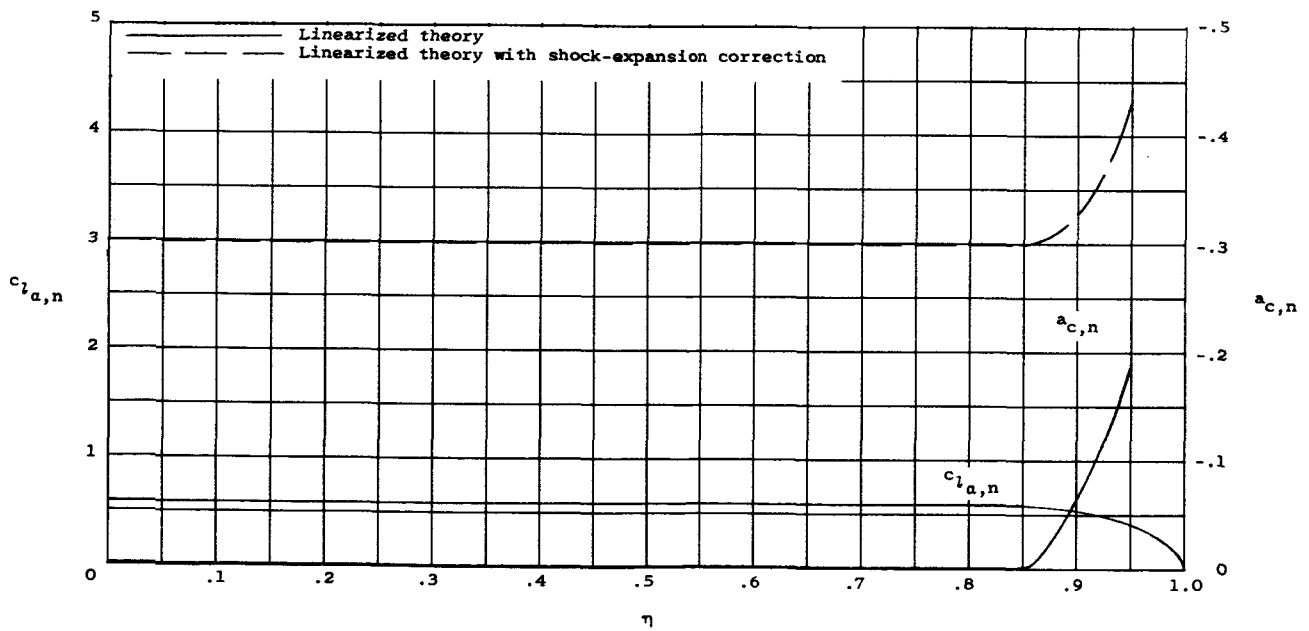


(n)  $M = 3.98$ .

Figure 4.- Continued.



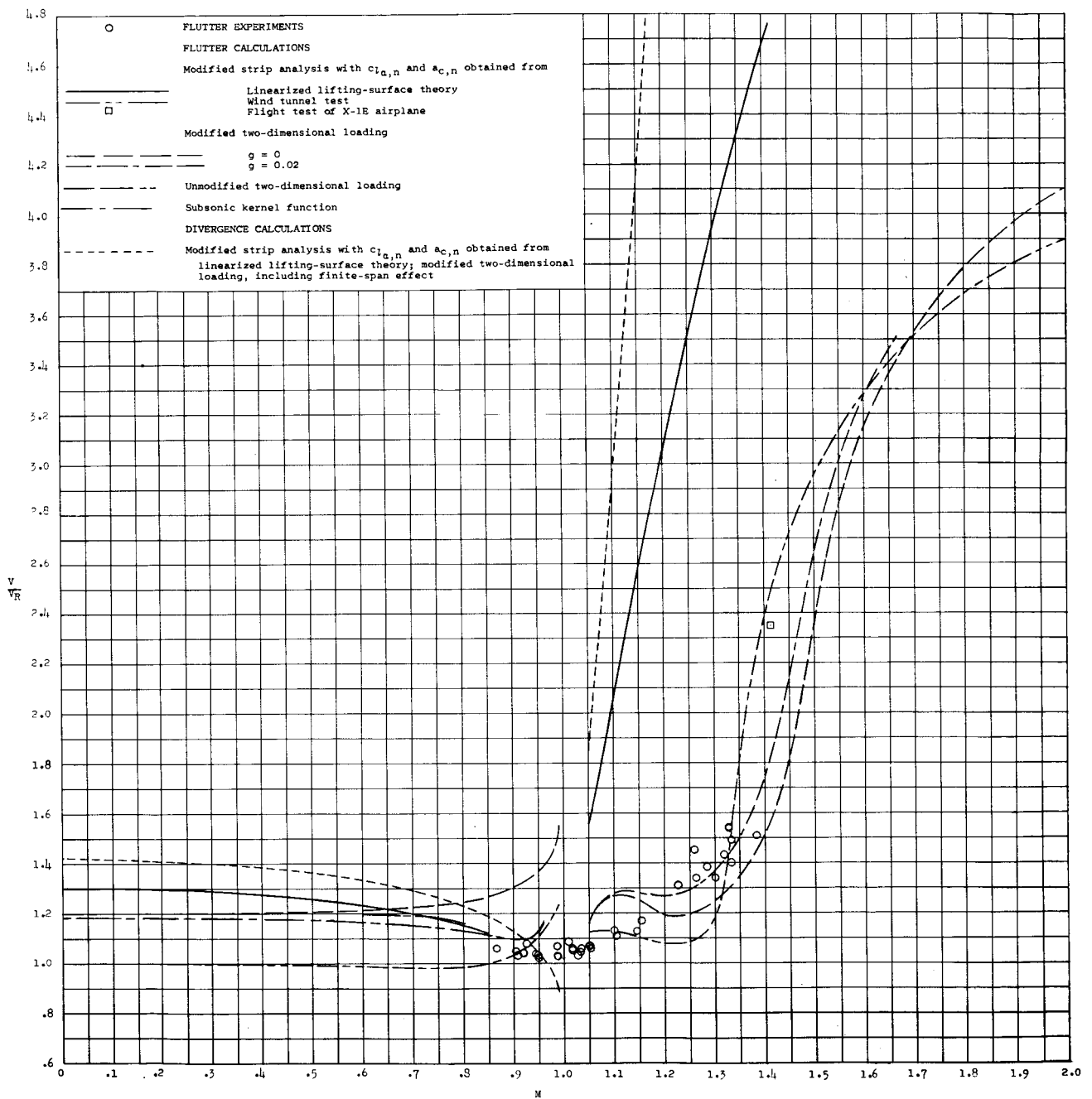
(o)  $M = 5.00$ .



(p)  $M = 6.86$ .

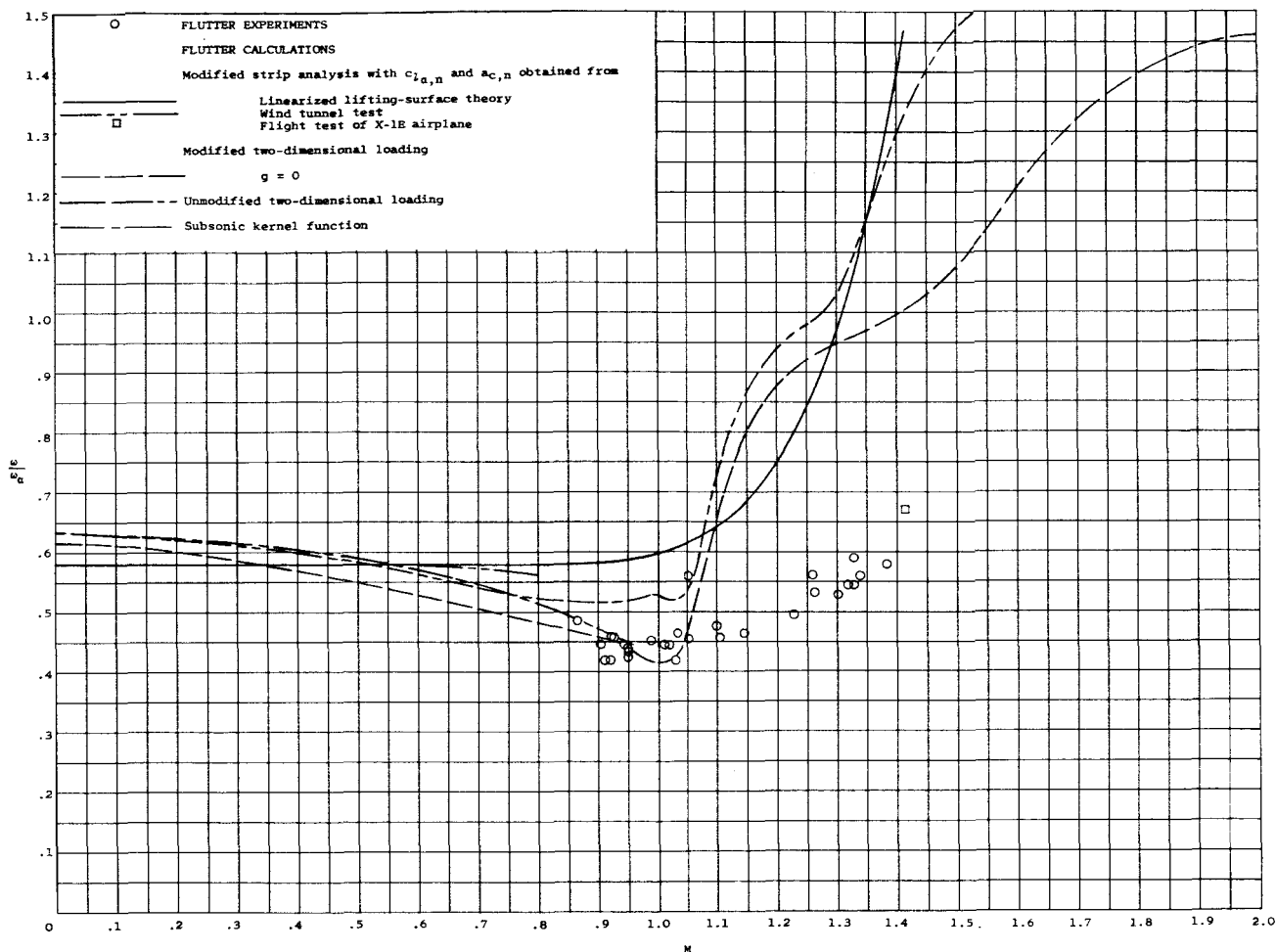
Figure 4.- Concluded.





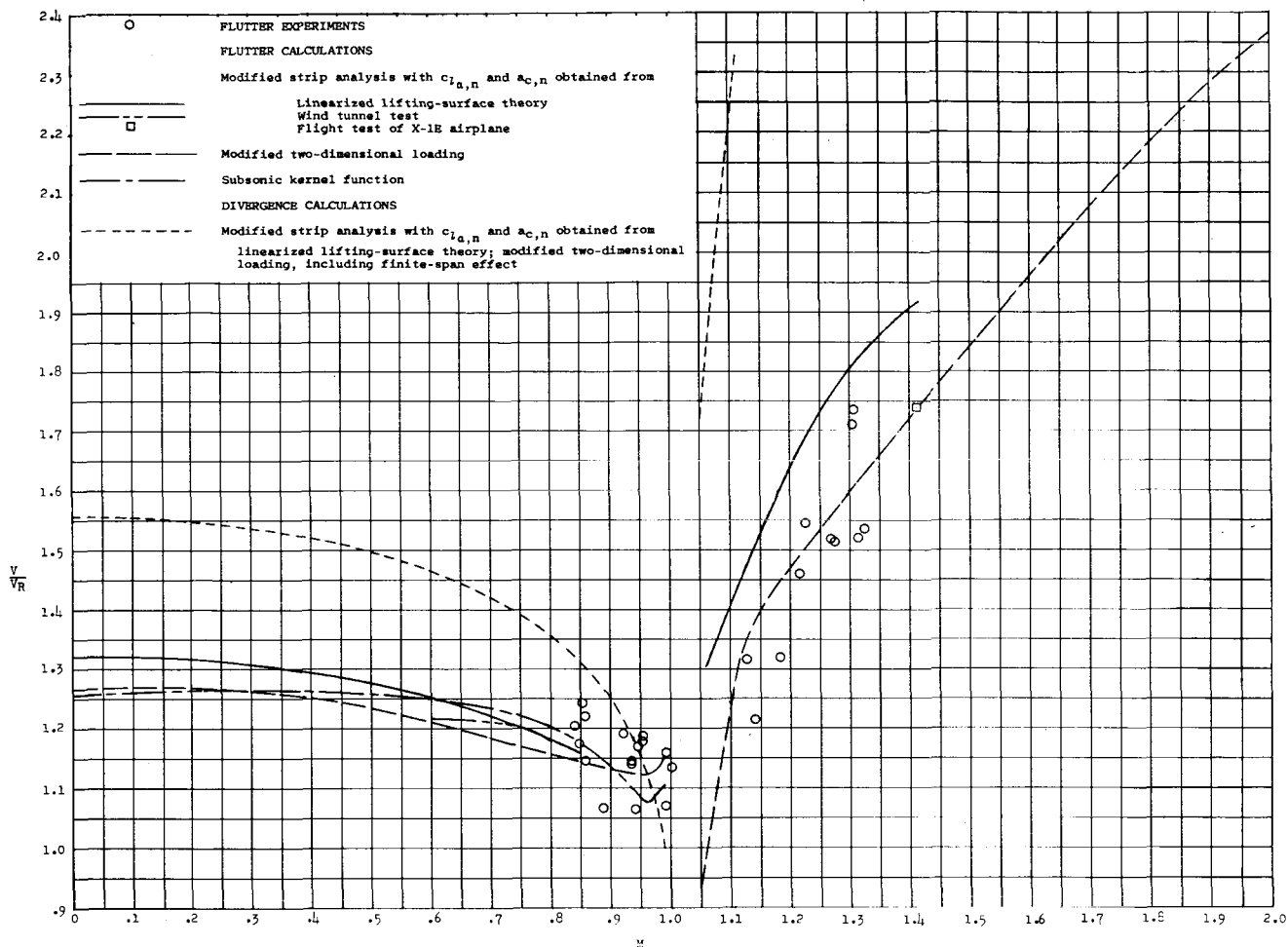
(a) Flutter-speed and divergence-speed ratios.

Figure 5.- Flutter and divergence characteristics of wing 400. For all calculated points  $\rho = 0.002378$  slug/cu ft,  $\omega_\alpha = 2,463$  radians/sec, and  $V_R = 976.5$  ft/sec.



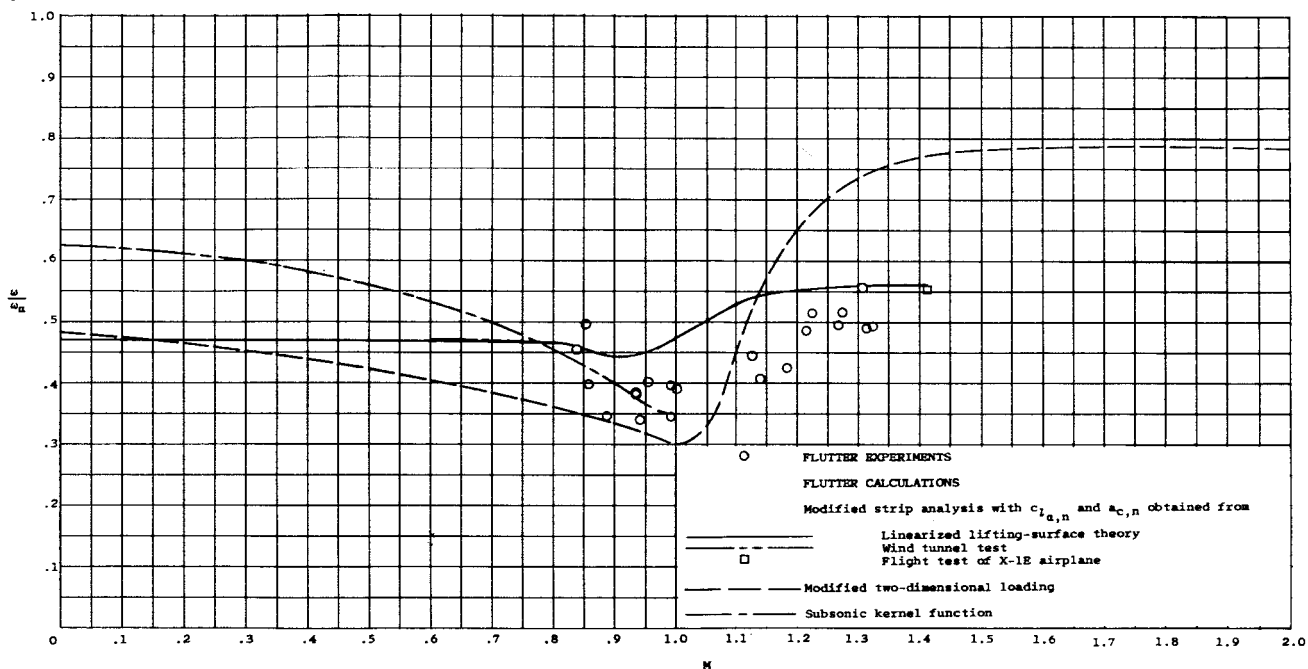
(b) Flutter-frequency ratios.

Figure 5.- Concluded.



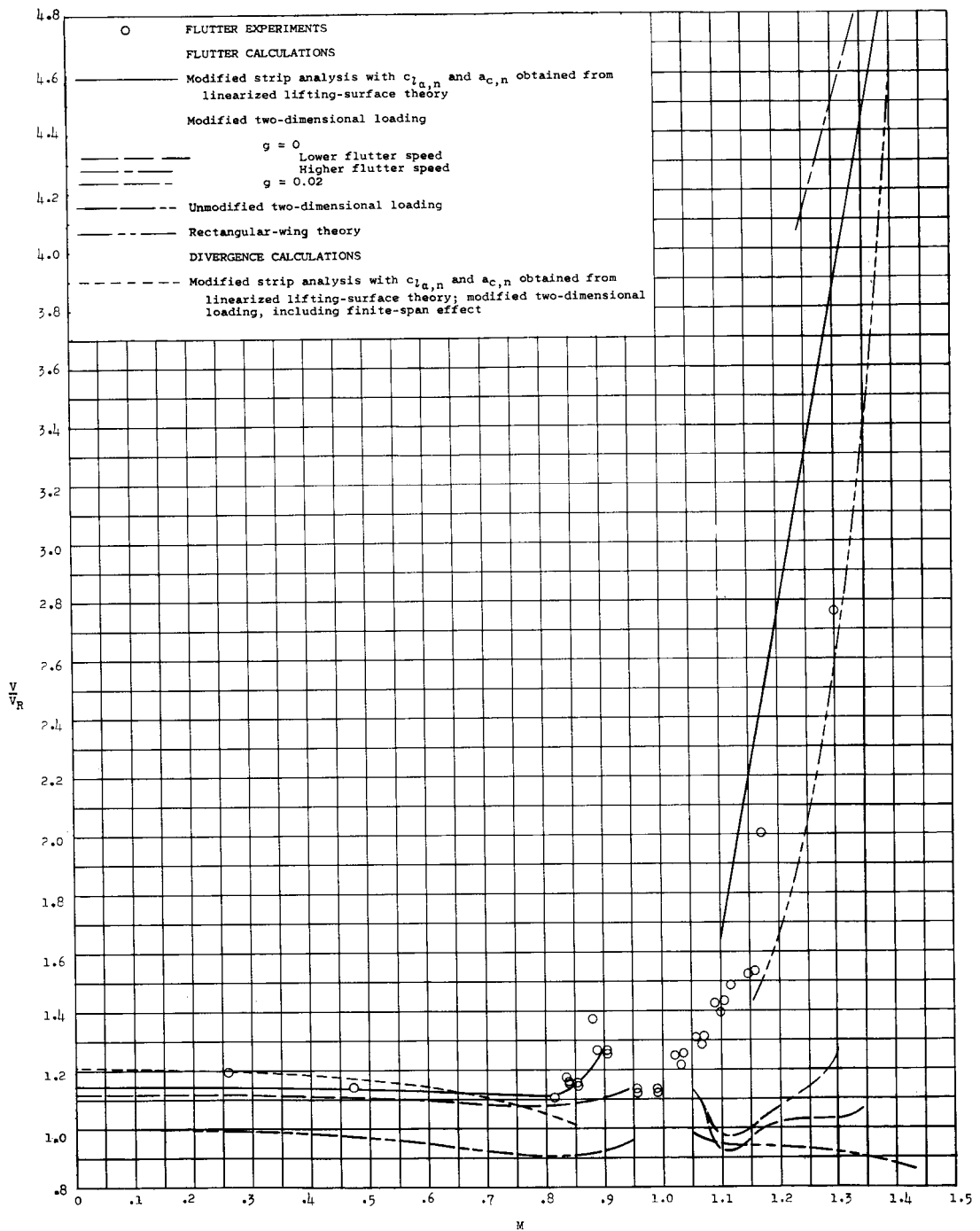
(a) Flutter-speed and divergence-speed ratios.

Figure 6.- Flutter and divergence characteristics of wing 400R. For all calculated points  $\rho = 0.003100$  slug/cu ft,  $\omega_\alpha = 1,982$  radians/sec, and  $V_R = 852.5$  ft/sec.



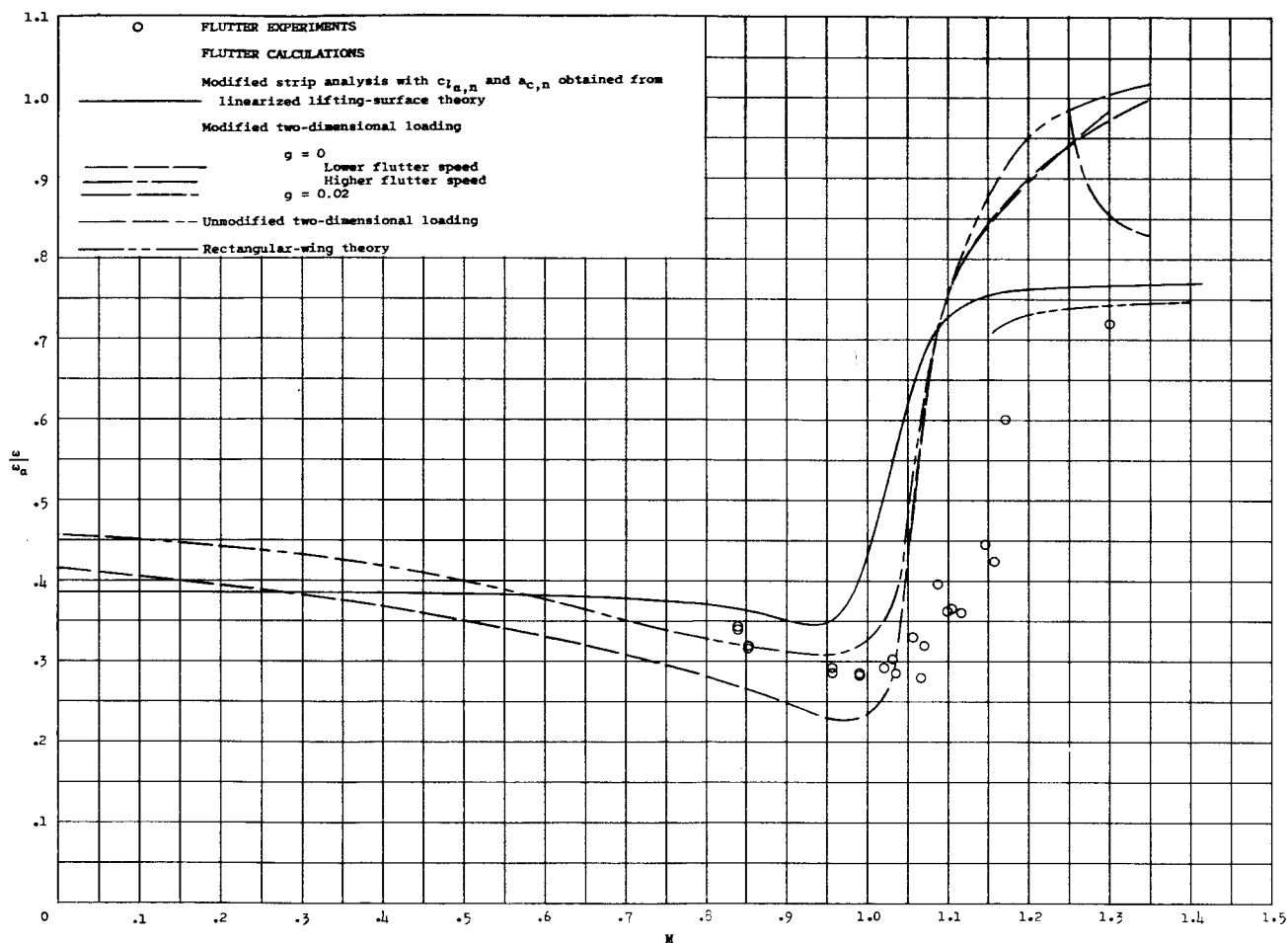
(b) Flutter-frequency ratios.

Figure 6.- Concluded.



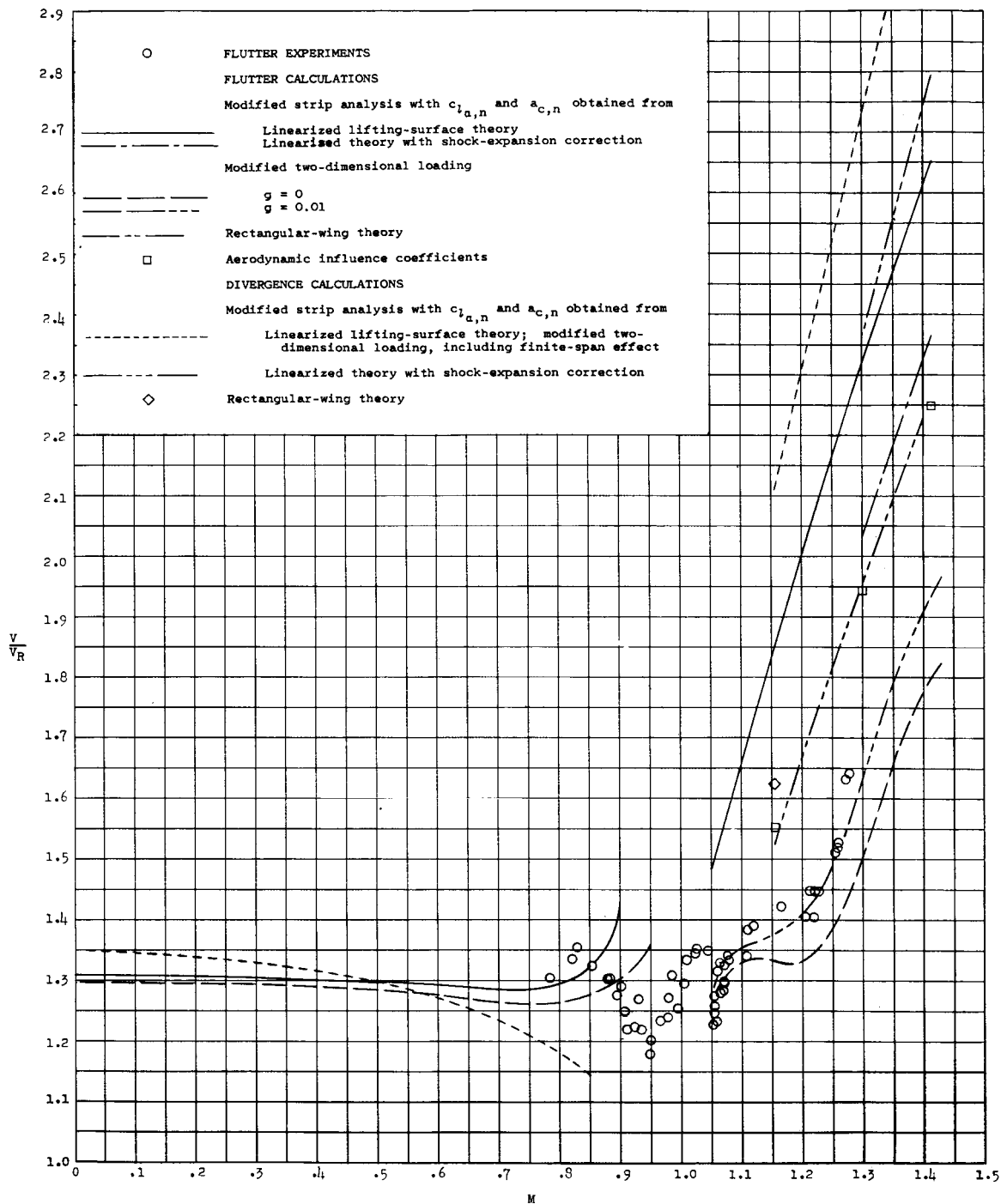
(a) Flutter-speed and divergence-speed ratios.

Figure 7.- Flutter and divergence characteristics of wing 7001. For all calculated points  $\rho = 0.005500$  slug/cu ft,  $\omega_\alpha = 2,271$  radians/sec, and  $V_R = 844.8$  ft/sec.



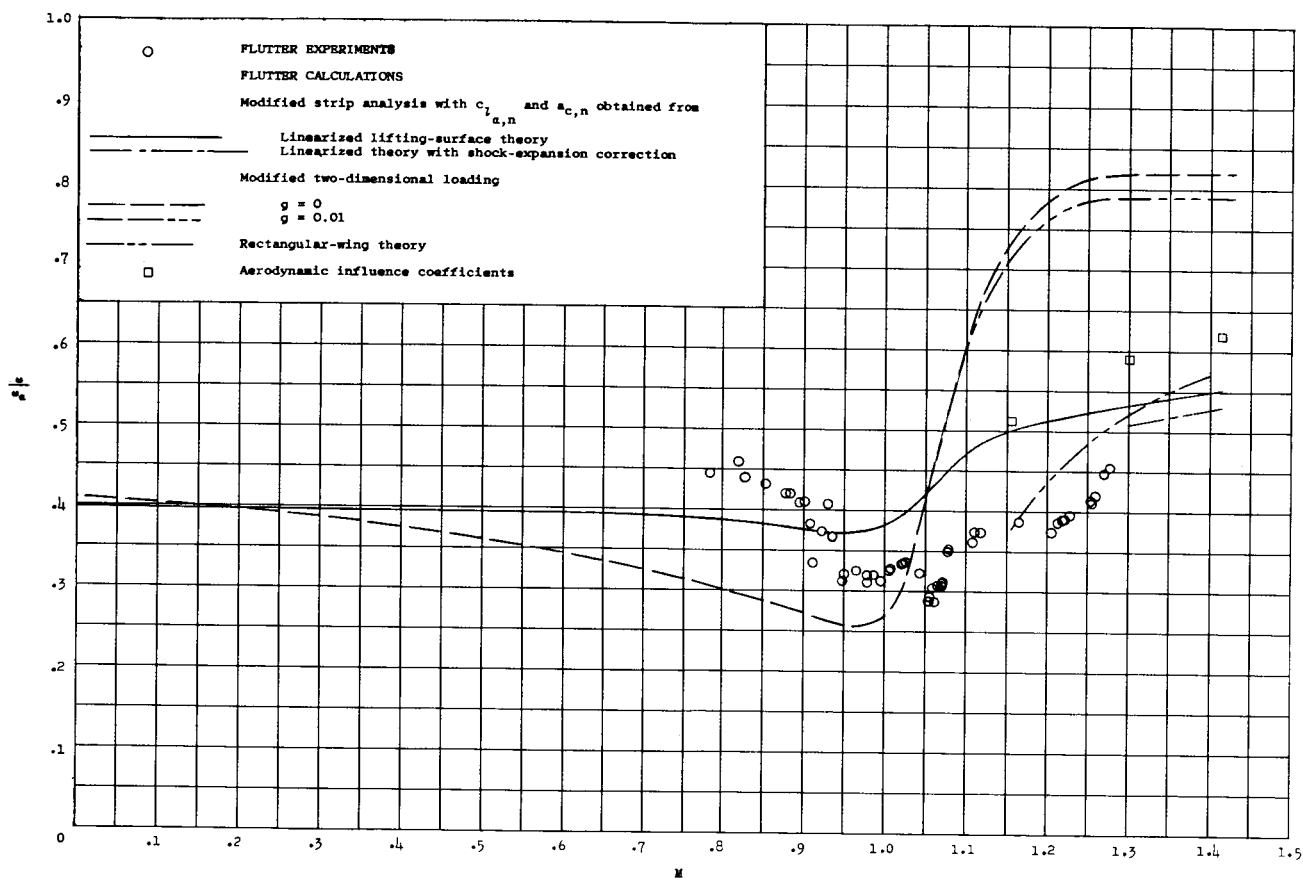
(b) Flutter-frequency ratios.

Figure 7.- Concluded.



(a) Flutter-speed and divergence-speed ratios.

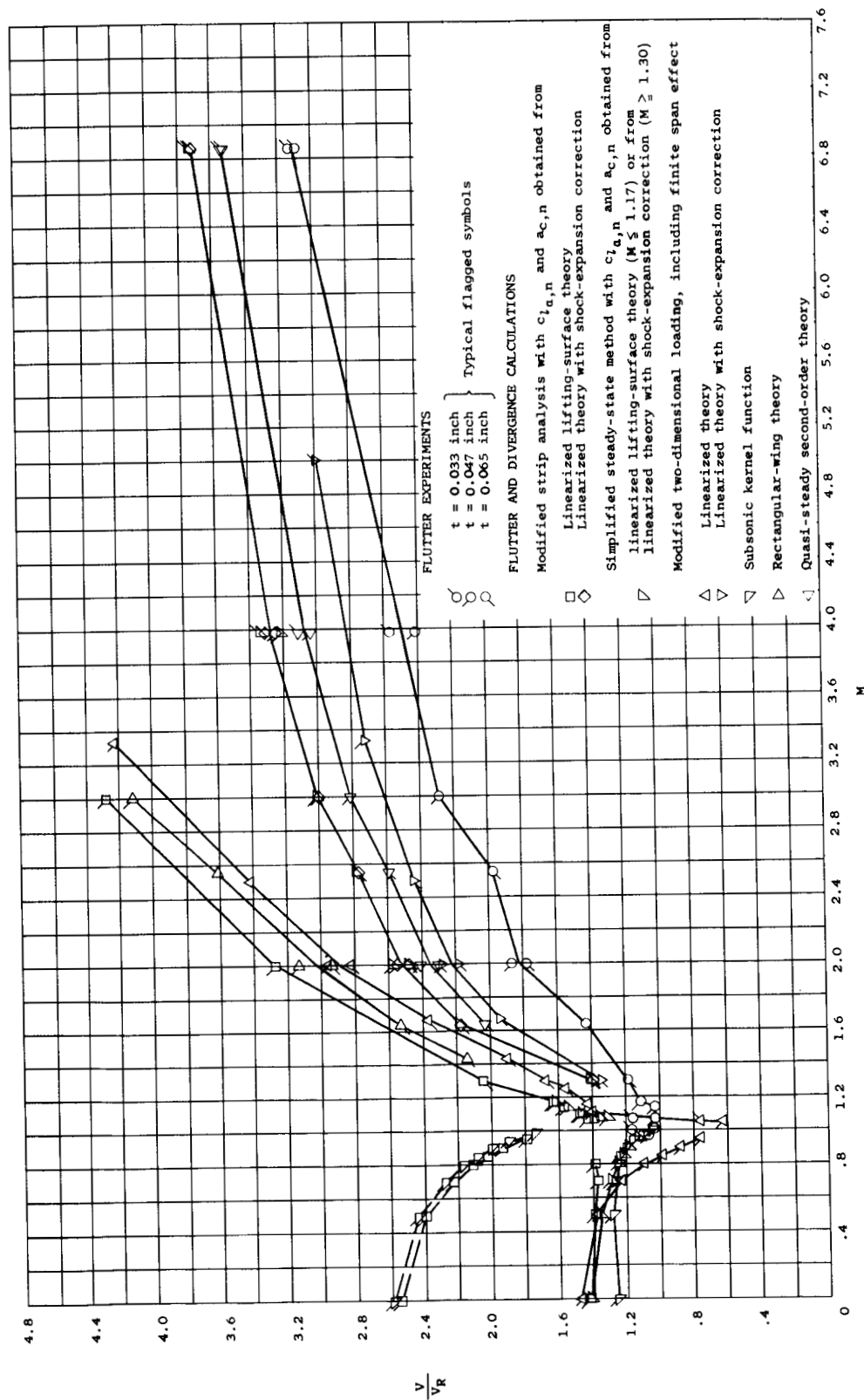
Figure 8.- Flutter and divergence characteristics of wing 4001. For all calculated points  $\rho = 0.002378$  slug/cu ft,  $\omega_a = 2,048$  radians/sec, and  $V_R = 828.5$  ft/sec.



(b) Flutter-frequency ratios.

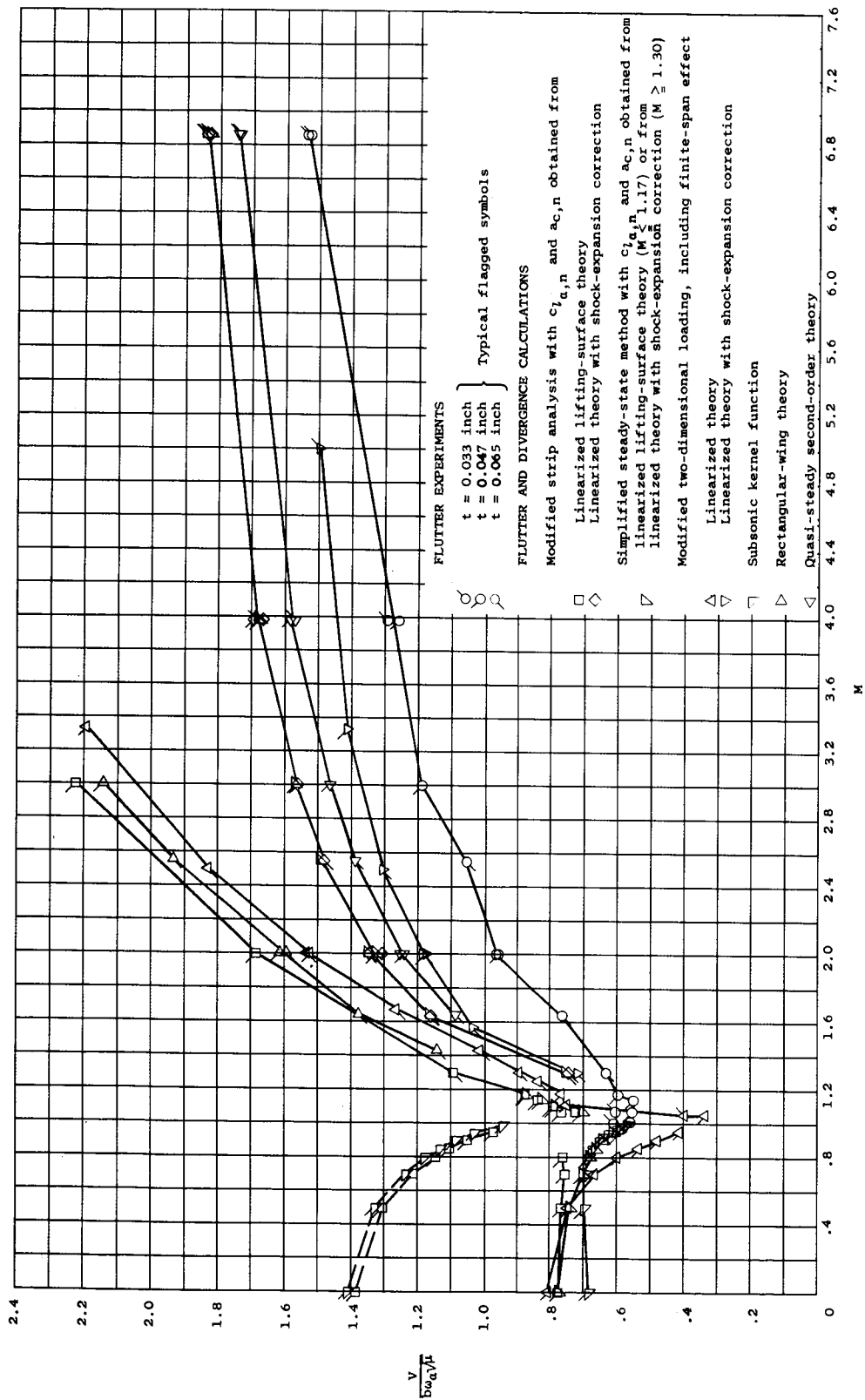
Figure 8.- Concluded.





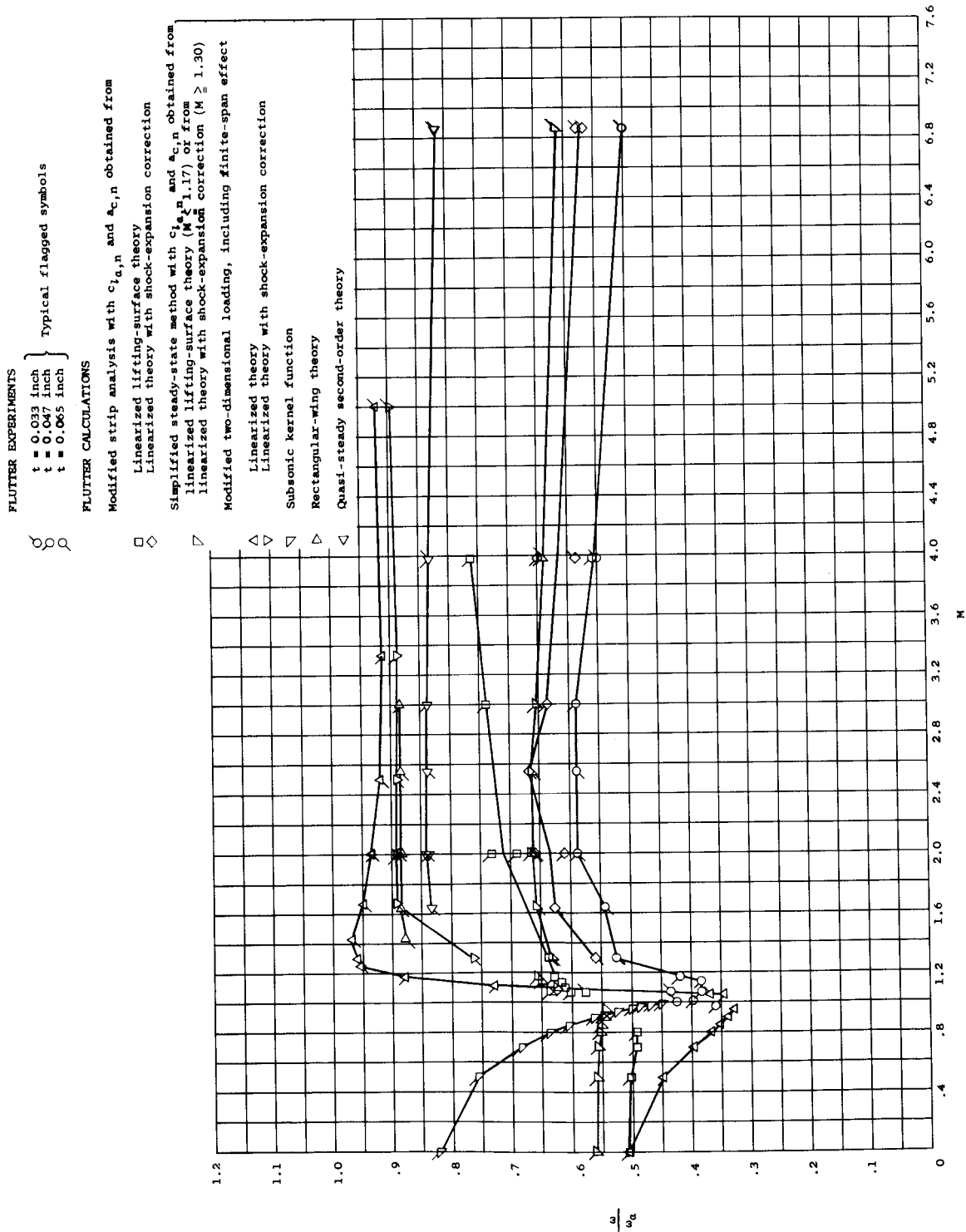
(a) Flutter-speed (solid lines) and divergence-speed (dash lines) ratios.

Figure 9.- Flutter and divergence characteristics of wing 2001. All calculations employed rigid-body vibration modes. For each calculation the value of  $\rho$  is that associated with the nearest experimental flutter point.



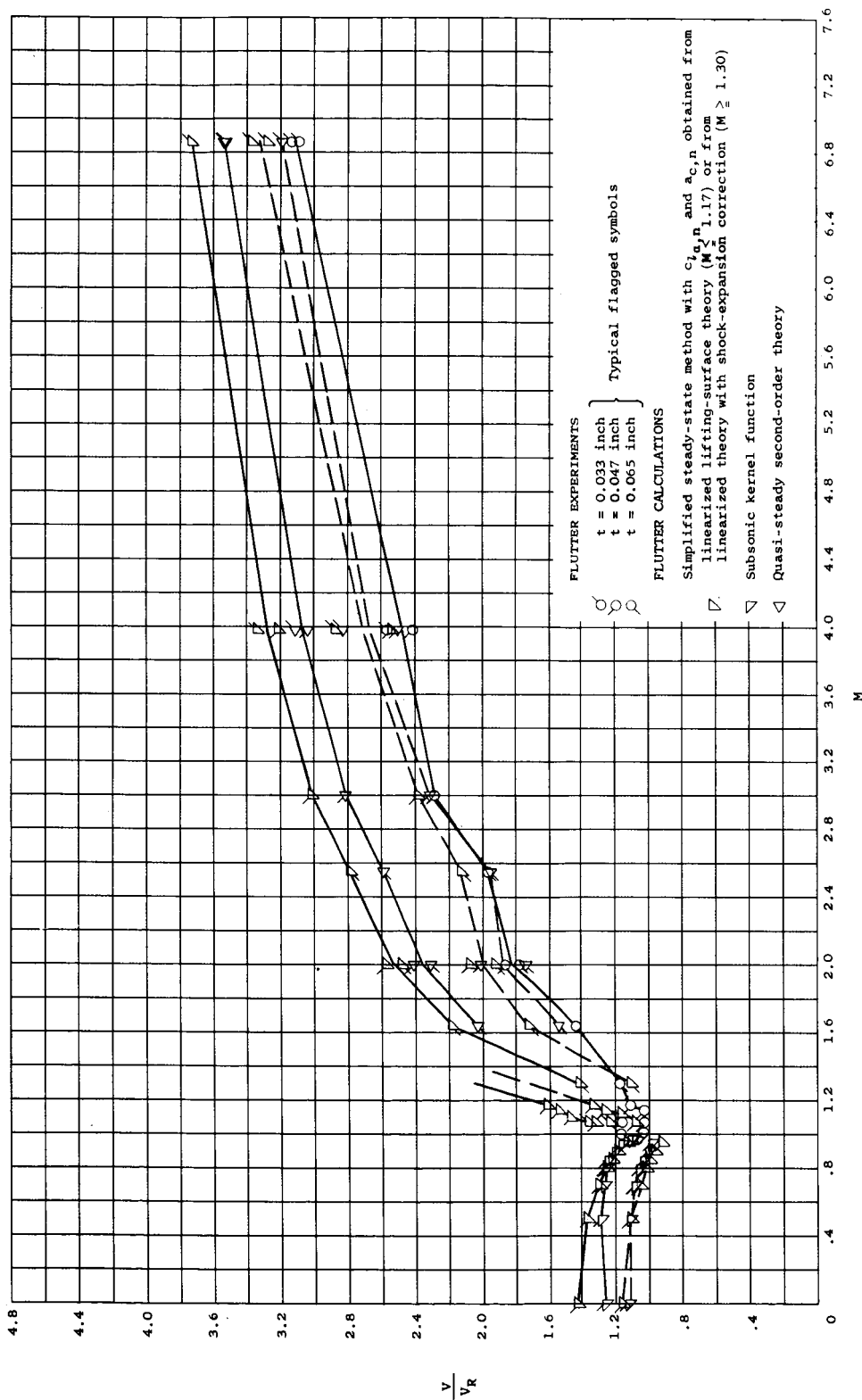
(b) Flutter-speed (solid lines) and divergence-speed (dash lines) indices.

Figure 9.- Continued.



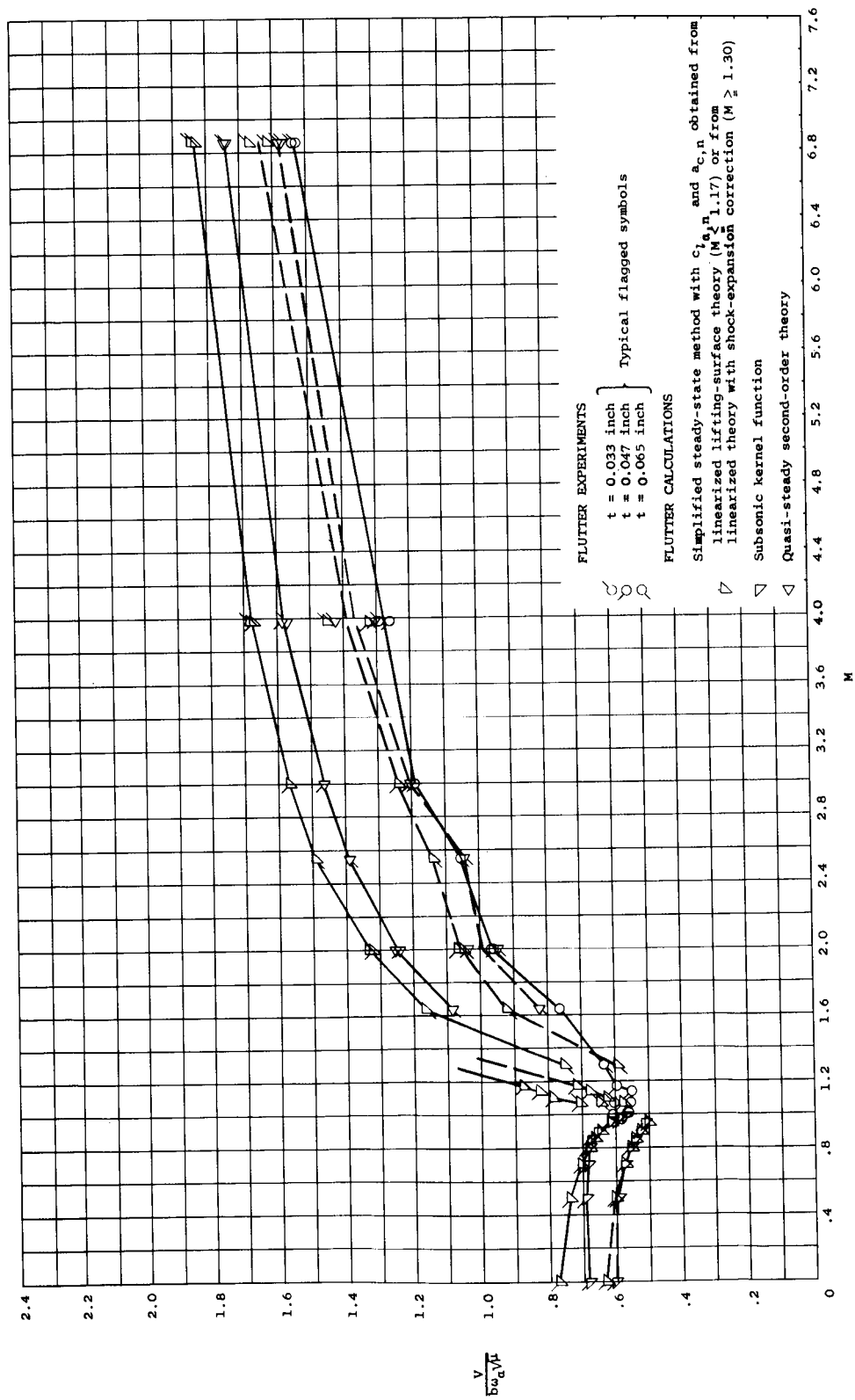
(c) Flutter-frequency ratios.

Figure 9.- Concluded.



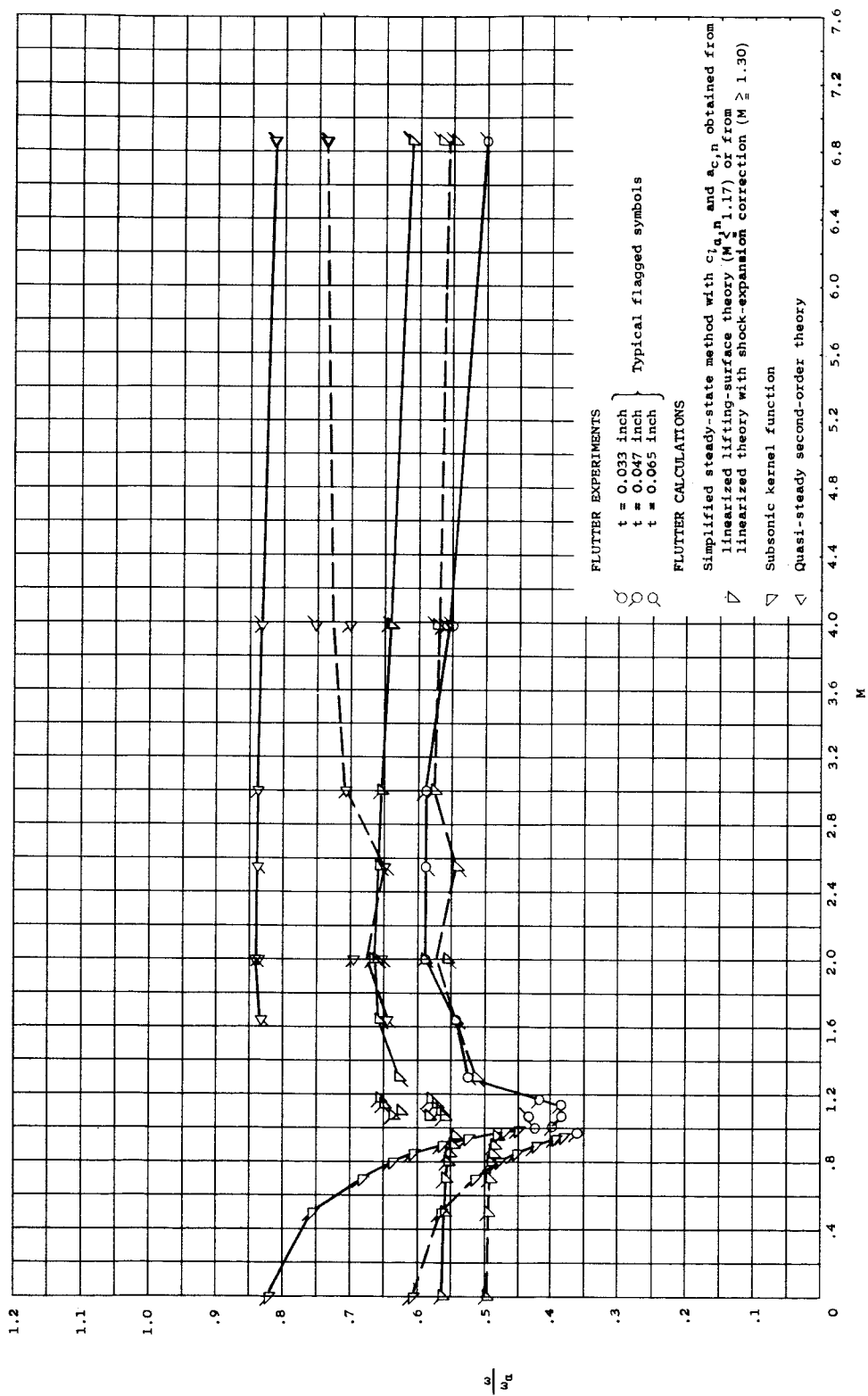
(a) Flutter-speed ratios calculated with rigid-body modes (solid lines) and with natural modes (dash lines).

Figure 10.- Flutter characteristics of wing 2001. Results of calculations employing rigid-body vibration modes and calculations employing natural vibration modes. For each calculation the value of  $\rho$  is that associated with the nearest experimental flutter point.



(b) Flutter-speed indices calculated with rigid-body modes (solid lines) and with natural modes (dash lines).

Figure 10.- Continued.



(c) Flutter-frequency ratios calculated with rigid-body modes (solid lines) and with natural modes (dash lines).

Figure 10.- Concluded.